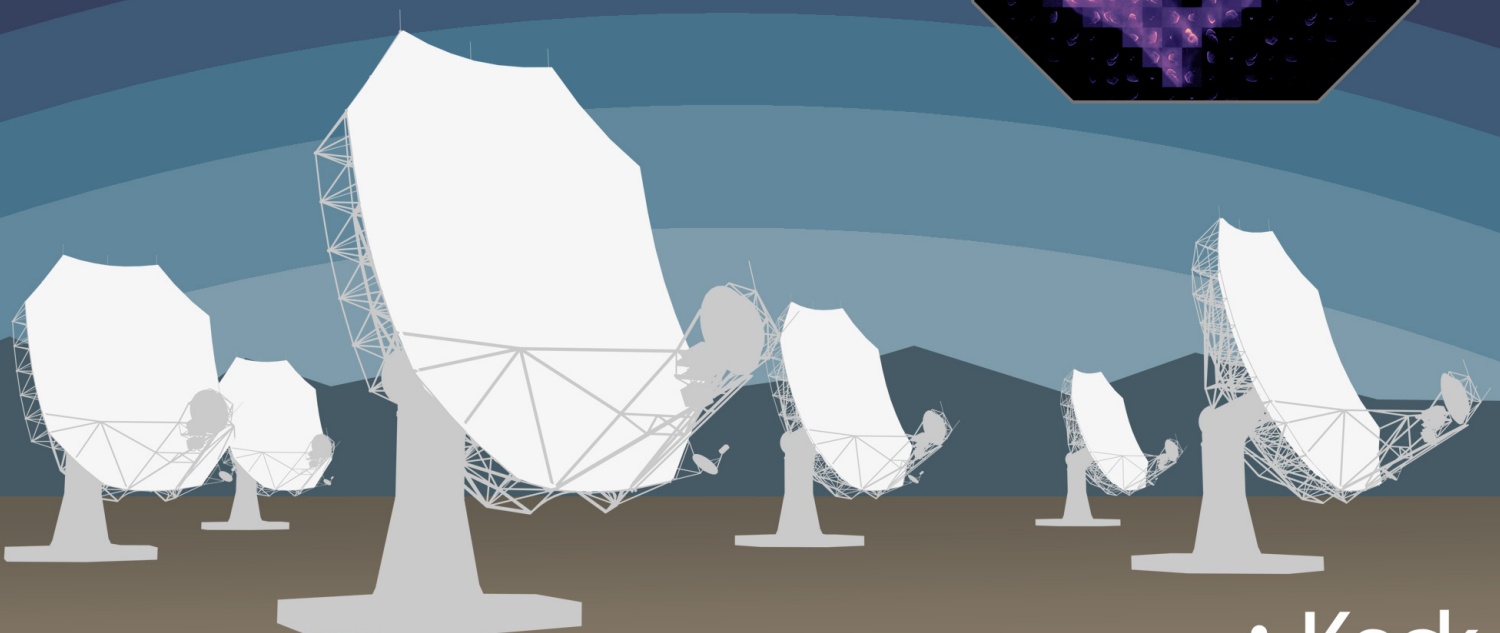
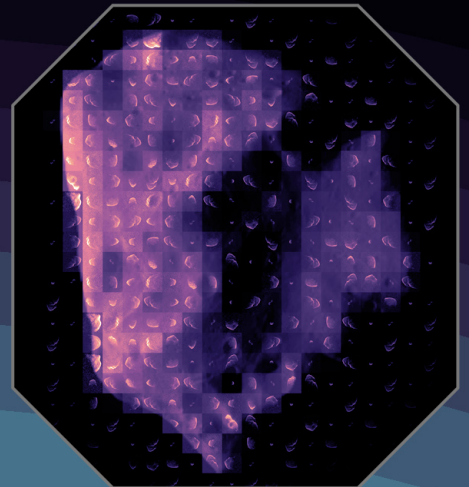
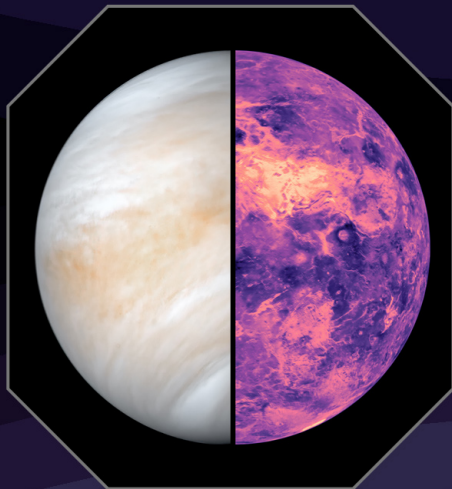
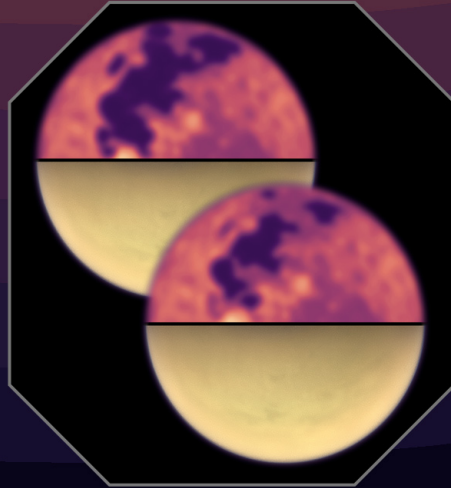


Next-Generation, Ground-Based **PLANETARY RADAR**



The Next-Generation Ground-Based Planetary Radar

Final Report prepared for the W. M. Keck Institute for Space Studies (KISS)
Jet Propulsion Laboratory, California Institute of Technology
<https://www.kiss.caltech.edu/programs.html#radar>

Recommended citation (long form):

Lazio, T. J. W., de Kleer, K., Ravi, V., Beasley, A. J., Benner, L. A. M., Bolin, B. T., Branson, D., Brozovic, M., Busch, M. W., Butler, B. J., Cambioni, S., Campbell, B. A., Campbell, D. B., Chodas, P., Kruzins, E., D’Addario, L. R., Gupta, H., Egan, M., Fast, K., Johnson, L., Marshall, S. E., O’Neil, K., Paganelli, F., de Pater, I., Pinilla-Alonso, N., Raymond, C. A., Rivera-Valentín, E. G., Roshi, A., Rubel, M., Stacy, N. J. S., Taylor, M., Taylor, P. A., Venditti, F. C. F., Vilnrotter, V. A., Virkki, A. K., Wilkinson, S., Vanderley, B. A. 2025, “The Next-Generation Ground-Based Planetary Radar,” report prepared for the W. M. Keck Institute of Space Studies (KISS), California Institute of Technology, eds. T. J. W. Lazio, K. de Kleer, & V. Ravi; doi: 10.26206/2jvv7-zjc89

Recommended citation (short form):

Lazio, T. J. W., de Kleer, K., Ravi, V., et al. 2025, “The Next-Generation Ground-Based Planetary Radar,” report prepared for the W. M. Keck Institute of Space Studies (KISS), California Institute of Technology; doi: 10.26206/2jvv7-zjc89

Study Workshop I: 2020 June 23–25

Study Workshop II: 2021 May 10–14



Study leads: Katherine de Kleer (California Institute of Technology), T. Joseph W. Lazio (Jet Propulsion Laboratory, California Institute of Technology), Vikram Ravi (California Institute of Technology),



Participants of the Next-Generation Ground-Based Planetary Radar workshop held virtually, 2020 June 23–25

Tony Beasley
National Radio Astronomy Observatory

Lance Benner
Jet Propulsion Laboratory, California Institute of Technology

Bryce Bolin
California Institute of Technology

Darrin Branson
USSPACECOM

Marina Brozovic
Jet Propulsion Laboratory, California Institute of Technology

Michael Busch
SETI Institute

Bryan Butler
National Radio Astronomy Observatory

Saverio Cambioni
University of Arizona

Bruce Campbell
Smithsonian Institution

Don Campbell
Cornell University

Paul Chodas
Jet Propulsion Laboratory, California Institute of Technology

Ed Kruzins
Commonwealth Scientific and Industrial Research Organisation

Larry D'Addario
California Institute of Technology

Harshal Gupta
National Science Foundation

Mike Egan
NASA/Science Mission Directorate

Kelly Fast
NASA/Science Mission Directorate

Lindley Johnson
NASA/Science Mission Directorate

Katherine de Kleer
California Institute of Technology

T. Joseph W. Lazio
Jet Propulsion Laboratory, California Institute of Technology

Sean Marshall
Arecibo Observatory/University of Central Florida

Karen O'Neil
Green Bank Observatory

Flora Paganelli
Green Bank Observatory

Imke de Pater
University of California, Berkeley

Noemi Pinilla-Alonso
Arecibo Observatory, Puerto Rico/University of Central Florida

Vikram Ravi
California Institute of Technology

Carol Raymond
Jet Propulsion Laboratory, California Institute of Technology

Edgard Rivera-Valentin
Lunar & Planetary Institute, USRA

Anish Roshi
Arecibo Observatory, Puerto Rico/University of Central Florida

Mike Rubel
Planet Labs, Inc.

Nick Stacy
Defence Science & Technology Group

Mark Taylor
Jet Propulsion Laboratory, California Institute of Technology

Patrick Taylor
Lunar & Planetary Institute

Flaviane Venditti
Arecibo Observatory/University of Central Florida

Victor Vlnrotter
Jet Propulsion Laboratory, California Institute of Technology

Anne Virkki
University of Helsinki

Steven Wilkinson
Raytheon Space and Intelligence

Bevin Ashley Zauder
National Science Foundation

“The Next-Generation Ground-Based Planetary Radar” study was made possible by the W. M. Keck Institute for Space Studies, and by the Jet Propulsion Laboratory, California Institute of Technology, under contract with the National Aeronautics and Space Administration.

The study leads gratefully acknowledge the outstanding support of Michele Judd, Executive Director of the W. M. Keck Institute of Space Studies, as well as the dedicated staff of KISS, who made the study experience invigorating and enormously productive, even in the depths of the COVID-19 pandemic. Many thanks are due to Tom Prince and the KISS Steering Committee for seeing the potential of our study concept and selecting it. We thank J. Wilsey for assistance with copy-editing and formatting of this report.

This research has made use of the Astrophysics Data System, funded by NASA under Cooperative Agreement 80NSSC21M00561. This research was supported by the National Aeronautics and Space Administration’s (NASA) Near-Earth Object Observations Program through grant 80NSSC19K0523 to the University of Central Florida (UCF). The Arecibo Observatory was a facility of the National Science Foundation. The Arecibo planetary radar program was fully funded by NASA. At the time of the workshop, the Arecibo Observatory was operated under a cooperative agreement with UCF, Yang Enterprises Inc., and Universidad Ana G. Méndez (UAGM). Part of this research was carried out at the Jet Propulsion Laboratory, California Institute of Technology, under a contract with the National Aeronautics and Space Administration.

Cover image: Robert Hurt(IPAC)/Keck Institute for Space Studies

Contents

	Executive Summary	ix
1	Introduction	1
2	Future Science Investigations	3
2.1	Inner Solar System	3
2.1.1	Venus	4
2.1.2	Mercury	5
2.1.3	The Moon, Mars and its Moons	6
2.2	Near-Earth Asteroids and Comets	7
2.2.1	Near-Earth Asteroids (NEAs)	7
2.2.2	Comets and Interstellar Objects	9
2.2.3	Planetary Defense	10
2.3	Main Belt Asteroids	12
2.3.1	Asteroid Families	12
2.3.2	Ice in the Main Belt	13
2.3.3	Interior Structures	14
2.3.4	Active Asteroids	14
2.4	Outer Solar System: Satellites and Small Bodies	15
2.4.1	Galilean Satellites	15

2.4.2	Titan	16
2.4.3	Other Satellites	17
2.4.4	Hildas, Trojans, and Centaurs	17
2.5	Science Case Requirements	18
3	Technical Concepts and Challenges	22
3.1	Summary of Current Capabilities	22
3.1.1	Speckle Analysis	25
3.1.2	Radar Interferometry	26
3.2	Future Capability: Ground-Based Single Antenna Radar Systems	26
3.2.1	Overview	26
3.2.2	The Path Forward	26
3.3	Future Capability: Ground-Based Radar Array	27
3.3.1	Calibration	28
3.3.2	Manufacturability	29
3.4	Space-Based Concepts	29
3.5	Cross-Cutting Considerations	30
3.5.1	Spectrum Management	30
3.5.2	Solid State Transmitters	30
3.5.3	Automation and Rapid Turnaround	32
3.5.4	Longitudinally-Spaced Transmitters and Global Coordination	34
3.5.5	Surveys	34
4	Ground-Based Planetary Radar Futures	36
A	Spacecraft Tracking	39



List of Figures

2.1	Ground-based Radar Observations of Sif Mons on Venus	4
2.2	Permanently-shadowed regions on Mercury identified with radar observations	5
2.3	Radar Images of Near-Earth Asteroids Acquired During the KISS Study	8
2.4	Radar Images of Comet Nuclei	9
2.5	Orbits of Potentially Hazardous Asteroids (PHAs)	11
2.6	Main Belt Erigone Asteroid Family Orbital Phase Space	13
2.7	Surface of Titan	16
2.8	Radar Detectability of Near-Earth Asteroids	18
2.9	Radar Accessibility of Solar System	19
3.1	International Planetary Radar Infrastructure	23
3.2	Demonstration Radar Arrays	27
3.3	Demonstration of N^2 Improvement in Equivalent Isotropic Radiated Power (EIRP)	28
3.4	Solid-State Radar Transmitters	32
A.1	Radar Tracking of Lunar Trailblazer	40



Executive Summary

Planetary radar observations have a laudable history of “firsts” including determining the astronomical unit with the precision sufficient for interplanetary navigation, water ice distribution at the Moon’s south pole, water ice indications in the permanently shadowed regions at Mercury’s poles, determining Venus’ rotation state, polar ice and anomalous surface features on Mars, indications that the asteroid (16) Psyche is an exposed metallic core of a planetoid, establishing the icy nature of the Jovian satellites, and the initial characterizations of Titan’s surface. In many cases, these discoveries made by planetary radar systems have motivated missions and mission radar instruments.

This W. M. Keck Institute of Space Studies study was intended to identify the compelling science and potential technical developments required for a next-generation, ground-based planetary radar. As new discoveries have occurred since the first generation of planetary radar observations, our understanding of the Solar System has improved, and new questions have emerged. One of the study’s motivations was to identify what discoveries might be enabled or how a next-generation planetary radar might address fundamental questions.

The study found that there are three compelling science drivers for a next-generation planetary radar—Venus, near-Earth asteroids, and the icy moons (“ocean worlds”) of the outer Solar System.

For Venus (“Earth’s evil twin”), long-term measurements of surface geology obtained with a planetary radar would provide context within which to interpret measurements from a suite of spacecraft planned to explore that planet over the next decade or more.

For near-Earth asteroids, an improved characterization of the population (or populations) would result from the increase in both the quantity of near-Earth asteroids that could be tracked and the quality of the data obtained. A planetary radar would provide precise orbit determinations for planning future spacecraft missions and assessing planetary defense hazards.

For the outer Solar System, much like for Venus, observations of icy moons/“ocean worlds” over unparalleled durations could be obtained, even enabling investigations of seasonal changes. Multiple additional science cases would be enabled, including potentially the tracking of interstellar objects, thereby bridging the fields of Planetary Science and Astrophysics.

A second motivation for this study was the two major ground-based planetary radar facilities were approaching their half-century anniversaries in 2023, with the Arecibo Observatory planning to celebrate its 60th anniversary of operations and NASA's Deep Space Network planning to celebrate the 50th anniversary of the start of construction of its Deep Space Station-14 (DSS-14) antenna, which hosts the Goldstone Solar System Radar (GSSR). Notably, and unfortunately, between the two workshops held as part of this study, the Arecibo Observatory collapsed.

This study found that a next-generation, ground-based planetary radar could be implemented as an antenna array, analogous to those already used in multiple radio astronomy facilities, which would provide greater resilience than a monolithic antenna.

Much of the technology for such a planetary radar array is maturing. A planetary radar array could be implemented with solid-state transmitters at each antenna, leveraging considerable commercial investments in solid-state technology and offering the promise of (much) more reliable performance than the traditional vacuum-tube klystrons. Solid-state transmitters have been prototyped and, in one case, deployed for spacecraft telecommunications.

Considerable promise exists to develop automation and new algorithms, even within existing systems, for both scheduling observations and processing planetary radar data.

Following this study, two more specific concept studies were conducted: "Cross-Disciplinary Deep Space Radar Needs Study" and "A Ground-Based Planetary Radar Array." Both reached similar conclusions: an array of 15–25 m diameter antennas equipped with 50–80 kW transmitters would be technically feasible and could address all compelling science cases identified in this report. A planetary radar array might even be capable of undertaking a survey designed to find near-Earth asteroids, a capability not currently available.



1. Introduction

Ground-based radar observations have probed all planets with solid surfaces and many smaller bodies in the Solar System (Ostro 2007; Virkki et al. 2023). Notable discoveries or findings include characterizing water distribution at the Moon's south pole (Stacy et al. 1997; Campbell et al. 2003a), the first indications of water ice in the permanently shadowed regions at Mercury's poles (Slade et al. 1992; Harmon et al. 1994), polar ice and anomalous surface features on Mars (Muhleman et al. 1991), providing crucial evidence supporting the icy nature of the Jovian satellites (Campbell et al. 1977; Ostro & Pettengill 1978), and initial characterizations of Titan's surface (Muhleman et al. 1990). This impressive and impactful work motivated science investigations on multiple space missions¹ including *Magellan*, *Cassini*, and *MESSENGER*, which carried radar as prime or co-prime instruments.

This W. M. Keck Institute for Space Studies study program was designed to assess the field's current state and explore future scientific and technical possibilities. Two major milestones drove the study. First, the Planetary Science & Astrobiology Decadal Survey, conducted under the auspices of the National Academies of Science, Engineering, & Medicine, was expected to commence, following on the *Vision & Voyages* (2013–2023) study. Second, both major facilities were nearing significant anniversaries in 2023. The Arecibo Observatory planned to celebrate its 60th year of operation, and NASA's Deep Space Network prepared to celebrate its 50th anniversary since construction began on Deep Space Station-14 (DSS-14), the home of the Goldstone Solar System Radar (GSSR).

Two KISS workshops were scheduled: 2020 June 22–26 and 2021 May 10–14. The interval between them proved more tumultuous than anyone could have anticipated. What began as an unusual pneumonia-like disease became recognized as coronavirus disease 2019 (COVID-19), and by 2020 March, it had developed into a global pandemic. As a result, both workshops were held entirely remotely. The adaptability and dedication of the KISS staff enabled them to rapidly pivot to virtual formats, ensuring both workshops could occur. Then, on 2020 December 1, the Arecibo Observatory collapsed,² destroying one of the world's two ground-based planetary radars. Finally, the

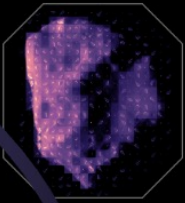
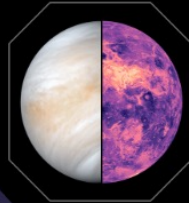
¹Ground-based radar observations in the late 1950s and early 1960s were critical to enabling interplanetary space missions simply to occur. Radar measurements of the distance to Venus enabled the determination of the astronomical unit to a sufficient precision that spacecraft could navigate over interplanetary distances.

²<https://new.nsf.gov/news/arecibo-observatorys-305-meter-telescope-suffers>

Planetary Science & Astrobiology Decadal Survey commenced, with a Statement of Task³ that, for the first time, required the survey to consider aspects of planetary defense.

The KISS workshops were structured to first define the science cases that would motivate an ambitious second half-century of ground-based planetary radar observations, and then to explore potential technical options to enable those observations. This report's structure largely follows the workshop structure, with Chapter 2 considering science investigations starting in the inner Solar System (Venus, Mercury, and the Moon), then moving outward through the Solar System to consider asteroids and the outer Solar System (beyond the Main Asteroid Belt). Chapter 3 describes a set of technical options and directions that could enable those ambitious science investigations. Reflecting on the long history of radar technology development, significant aspects of developing new ground-based planetary radars focus on system engineering and integration rather than developing entirely new technologies. Chapter 4 summarizes the landscape and potential future directions since the conclusion of the second workshop.

³<https://www.nationalacademies.org/our-work/planetary-science-and-astrobiology-decadal-survey-2023-2032>

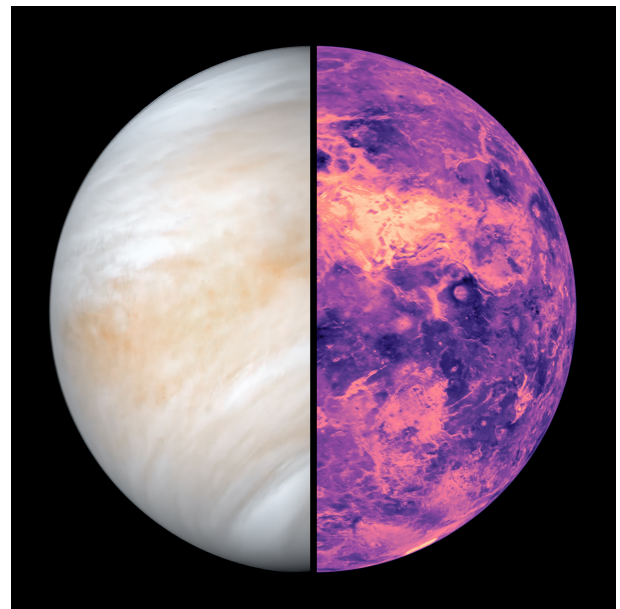


2. Future Science Investigations

This chapter outlines the range of scientific investigations that future ground-based planetary radars could enable, including making the discoveries that would enable the development of missions to conduct more detailed investigations. Section 2.1 considers the potential opportunities associated with studying the terrestrial planets, including the Moon. Section 2.2 focuses on observing near-Earth objects, which interest both planetary science and planetary defense communities. Section 2.4 illustrates the significant returns that radar observations targeting the outer Solar System would provide. Section 2.5 assembles a notional set of science requirements for a future ground-based planetary radar based on the discussions in the previous sections.

2.1 Inner Solar System

We are in an era when obtaining spacecraft-quality data from ground-based facilities is possible. Ground-based radar critically supports studying planetary surfaces and prepares for spacecraft missions, complements active missions, and can continue investigations after missions end. Among the inner Solar System bodies, Venus drives the main science case for a next-generation planetary radar, with specific technological demands for studying its surface. Mercury presents a strong science case, yet is attainable with the radar capabilities required for other science (such as Venus or asteroids), while the Moon and Mars serve ancillary roles since they can benefit from the capabilities required to meet the science goals for Venus and Mercury.



Planetary radar reveals Venus's normally cloud-obscured surface.

2.1.1 Venus

With an optically-opaque atmosphere 90 times Earth's density, detailed Venus surface mapping remained impossible until high-power radar systems became available at Arecibo and Goldstone in the early 1970s. Arecibo collected the finest resolution Earth-based measurements from 1988 through 2020, which resolved features at about the kilometer scale.

Even with near-global radar image coverage by the Magellan mission, current geologic activity levels remain essentially unknown due to Magellan's short time scale and finer resolution relative to ground-based observations. Hints of recent volcanism come from atmospheric gas measurements, near-infrared emission maps, and identification of features typical of volatile-rich eruptions. Since the workshop, NASA and ESA have selected two orbital radar mapping missions, NASA's Venus Emissivity, Radio Science, InSAR, Topography, and Spectroscopy (VERITAS) and ESA's EnVision, to study Venus, with planned arrival at the planet in the early to mid-2030s. Collectively, the mission goals are to better understand the distant history of the crust and the modern processes and locations of volcanic activity. Next-generation planetary radars will complement both missions.

VERITAS and EnVision will provide high-resolution images, topographic maps, and perhaps interferometric surface deformation measurements across Venus. Even with these important datasets, Earth-based mapping plays a vital role because of its much longer temporal coverage and roughly 20 month cadence. The current base of kilometer-scale maps produced by Arecibo extends across 32 years (Campbell & Campbell 2022). While limited to a single hemisphere of Venus visible at inferior conjunction, this time base allows comparison with those of orbital missions with lifetimes of three to four years, spaced 40 or more years apart.

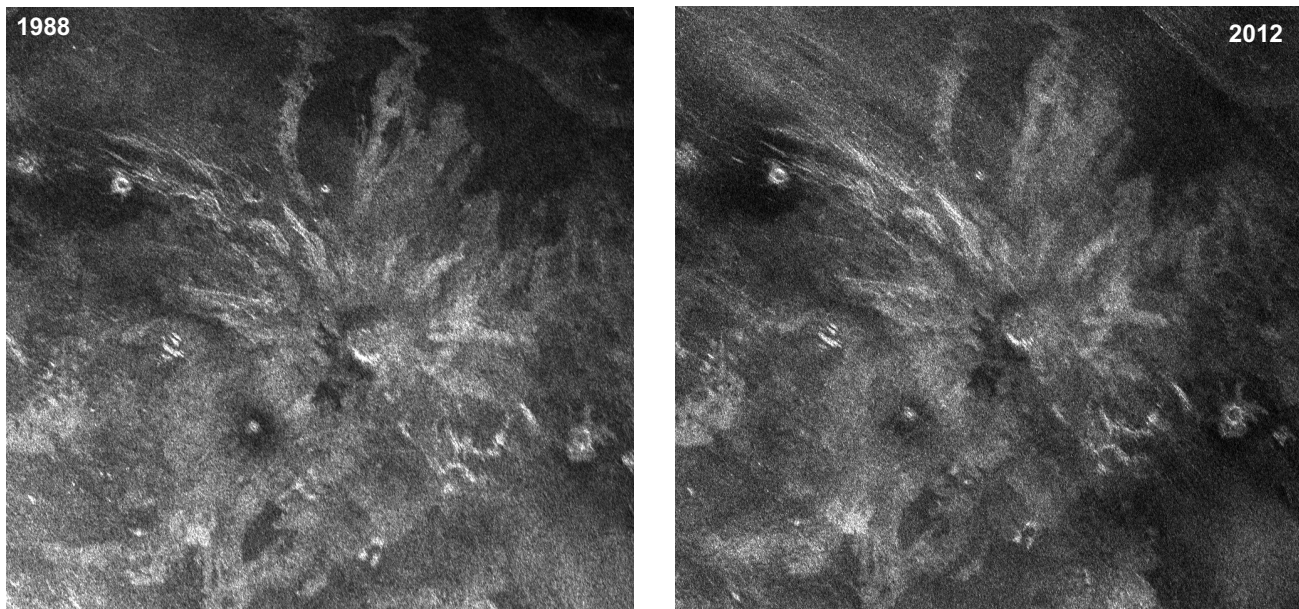


Figure 2.1: Ground-based radar observations of Venus' surface can span multi-year to multi-decade time scales, allowing changes due to volcanic lava flows to be detected and monitored. These radar images of Sif Mons acquired in 1988 and 2012 have identical viewing geometries, allowing possible changes to be identified. (Credit: B. Campbell)

A steady cadence of Earth-based observations, coupled with improved instruments and power, provides a strong argument for expanding and enhancing Venus radar programs. Understanding volcanic processes on Venus requires a combination of orbital data and Earth-based radar mapping. Ahead of a new mission, Earth-based data may identify candidate large ($>100 \text{ km}^2$) new flow features; for reference, the Kilauea volcano produced a flow feature covering 144 km^2 in 35 years. Orbital radar and infrared observations can verify these results and identify young, unweathered

material and the flow outline that has occurred since the Magellan mission (≈ 40 years earlier by the time that VERITAS and EnVision reach Venus). A single mission can thus confirm and catalog numerous likely recent events, but will not follow up on these results with long-duration monitoring.

Developing a higher-resolution Earth-based capability similar to orbiting spacecraft and signal processing methods for imaging farther from inferior conjunction would leverage orbital mission results toward a more complete view into Venus' hidden surface processes. A radar system operating in the L- to S-band range (1 to 3 GHz) can meet these goals, which is a requirement in light of rapid absorption increases by Venus' atmosphere for higher frequencies. With Arecibo's collapse, there are *no* Earth-based planetary radar assets available to study Venus' surface in detail. Next-generation planetary radar transmitting and receiving capabilities should be sufficient to achieve $1\ \mu\text{s}$ time resolution that will provide image resolutions around 150 m, about 10 times finer than previous ground-based radar and comparable to Magellan, allowing for comparison on hemispheric to near-global scales. These measurements achieve full value only when an array receives the signal and resolves north-south ambiguity in delay-Doppler imaging. Signal processing techniques and higher power will also enhance surface coverage by allowing imaging farther in time from inferior conjunction.

Improved optical image resolution has expanded knowledge about Mars' ancient past. Similarly, only a robust program combining orbital and Earth-based radar observations will answer key questions about Venus' geologic history and water's role in the distant past.

2.1.2 Mercury

After determining Mercury's correct rotation rate (Pettengill & Dyce 1965), the next notable ground-based, radar-enabled discovery was the identification of radar-bright features at its poles (Slade et al. 1992; Harmon & Slade 1992). Scattering models suggested that these features were due to the presence of water ice (Butler et al. 1993). NASA's MESSENGER spacecraft confirmed that these radar-bright features are typically associated with permanently shadowed regions (PSRs, Chabot et al. 2012; Deutsch et al. 2016) that are, on average, hydrogen-rich (Lawrence et al. 2013). However, Figure 2.2 shows that further analysis revealed many PSRs at the north pole lack radar-bright deposits (Deutsch et al. 2016). This could imply that not all cold traps are occupied, which would provide constraints on volatile timing and volume, either exogenically delivered to Mercury or released during volcanic outgassing.

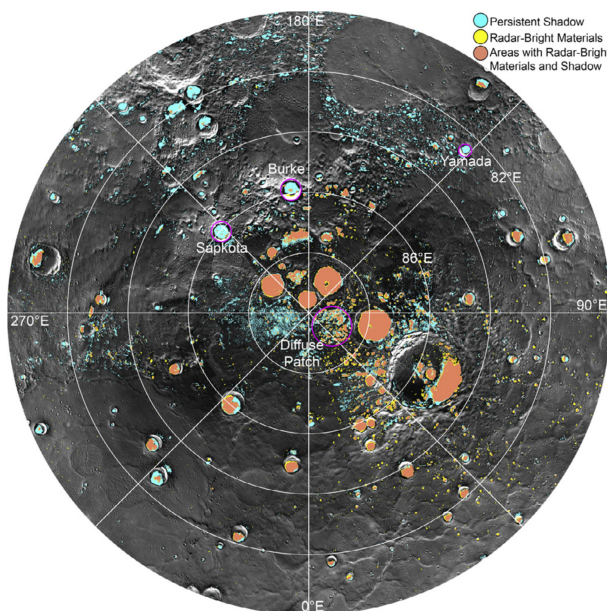


Figure 2.2: Polar stereographic view of Mercury's North Pole, noting areas in permanent shadow, as derived from high-resolution MESSENGER data (cyan), areas with a radar-bright return (yellow), and areas where radar-bright features are collocated with a permanently-shadowed region (PSR, orange). Sapkota and Burke craters are highlighted as large PSRs missing a radar-bright feature. Craters with a radar-bright return not associated with a PSR location are typically smaller.

[Reprinted from *Icarus*, Vol. 280, Deutsch et al., "Comparison of areas in shadow from imaging and altimetry in the north polar region of Mercury and implications for polar ice deposits," pp. 158–171, Copyright (2016), with permission from Elsevier]

Some radar-bright features are not collocated with PSRs, which could indicate transient water ice deposits or scattering due to other regolith physical properties. Full radar mapping, particularly at multiple wavelengths, such as at S- and X band (2 GHz to 9 GHz), paired with radar scattering models informed by MESSENGER data, would improve the characterization of Mercury’s polar volatiles. Resolving the distribution and quantity of ice at Mercury provides valuable insights into its geologic history and surface evolution and helps resolve volatile delivery and transport on other airless bodies, such as the Moon.

Considering the BepiColombo mission to Mercury (planned orbit insertion in 2026 November), further characterizing Mercury’s surface is timely and provides synergy with mission objectives. Early Arecibo radar observations revealed the prominence and variety of fresh impact craters and their ray systems (Harmon et al. 2007), but much more remains to be done to characterize the planet’s smooth plains, volcanic deposits, and inter-crater plains, including their compositions (e.g., radar loss tangents), relationship to impact structures, and emplacement histories. MESSENGER’s extensive geological and compositional information provides excellent context that can help better decipher radar products, and untangle degeneracies in radar scattering models (e.g., Rivera-Valentín et al. 2021; Rivera-Valentín et al. 2022). Continued radar observations are complementary to spacecraft data and can facilitate future landed missions (Rivera-Valentín et al. 2020).

Mercury’s size and rotation create a moderately overspread target for delay-Doppler imaging at S band ($F = 1.1$ – 1.7 , where F is the echo dispersion factor). This requires using the long-code method to adequately partition the target echo into delay-Doppler cells (Harmon 2002). Moreover, given that the primary observing targets are at Mercury’s poles, a ground-based radar sensitive enough to result in high signal-to-noise ratios at high incidence angles is required. Since target craters are kilometer-scale, the system also needs a resolution finer than 1 km. Monostatic radar observations using the Arecibo Observatory were uniquely suited for such observations. Continued Mercury radar studies require an equivalent or improved system.

2.1.3 The Moon, Mars and its Moons

Radar imaging has a long history of the Moon, at wavelengths from a few centimeters to several meters. With the loss of the Arecibo Observatory, high-resolution Earth-based capability exists primarily at Goldstone. A short-wavelength (few centimeter) radar system may be installed on the Green Bank Telescope, and technology demonstrations have produced meter-scale resolution lunar images (§3.2.2). Lunar orbital radar data have grown tremendously in the past 20 years, most recently with fully polarimetric L- and S-band coverage from Chandrayaan-2. Global coverage requirements and favorable polar viewing geometries clearly favor orbital systems.

One unique niche in which Earth-based lunar radar excels lies in longer wavelengths than orbital systems presently use. Arecibo’s 430 MHz signals could reach the lunar regolith base in some regions, and to 30 m depths or more in the lunar highland soil. Atmospheric and ionospheric facilities have studied the Moon, such as the Jicamarca system at 50 MHz (6 m wavelength, Vierinen et al. 2017). The EISCAT 3D at 233 MHz (1.3 m wavelength) may also image the Moon with significant depth penetration in the future. The major scientific rationale for new Earth-based long-wavelength or very short-wavelength radar lunar observations requires additional development.

Earth-based Mars observations with the Arecibo S-band system and Goldstone provided stunning detail showing lava flow complexes hidden by surface dust, and gave the first indication of a unique “Stealth” region still poorly understood (Muhleman et al. 1991; Harmon et al. 2012). Two outstanding Mars questions that a next-generation, ground-based planetary radar system could address are:

- The upper polar cap layer characteristics, which are known to be complex and seasonally varying, and
- The lava flow roughness, spatial extent, and water-carved features beneath the pervasive dust cover.

In both cases, L- to S-band capabilities proposed for Venus observations would enable these studies.

The Mars science plan carries one significant caveat. If the International Mars Ice Mapper (IMM, Baker et al. 2024) mission flies with an L-band orbital radar system with full polarimetry, it would remove the niche available to

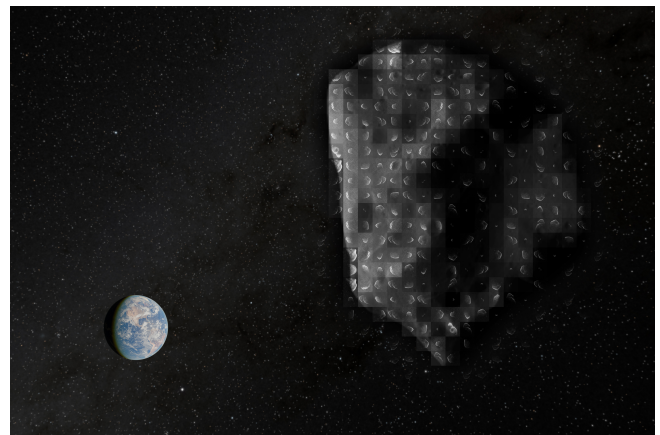
ground-based radars studying Mars. Unlike Venus, long-time scale observation requirements are less compelling for Mars, where large-scale surface geological activity is not suspected.

A next-generation planetary radar built specifically to observe Venus and/or small near-Earth asteroids or kilometer-scale Main Belt asteroids could provide similar Martian moon observations targeting Phobos and Deimos.

Previous Phobos and Deimos observations have provided surface property information (Ostro et al. 1989; Busch et al. 2007), and continuing such observations in the future would complement measurements that the upcoming Martian Moons eXploration mission (MMX, Genda et al. 2024) will obtain. Radar monitoring also would provide astrometry and updated orbit fits for the moons independently from Mars-orbiting spacecraft.

2.2 Near-Earth Asteroids and Comets

Planetary radar observations not only provide essential information about the nature of near-Earth asteroids, they are a critical element of planning spacecraft missions to such objects and for planetary defense. Planetary radar measurements obtain orbital information that is complementary to the visible and near-infrared wavelength observations with which near-Earth asteroids are discovered. This orbital information can then be used to identify which objects are suitable for being targets of spacecraft missions and assessing impact hazards. Planetary defense is integrally coupled to the science measurements.



2.2.1 Near-Earth Asteroids (NEAs)

Radar provides a powerful tool for studying both physical and dynamical near-Earth asteroid (NEA) properties. The total radar-detected NEA count¹ exceeds 1000, enabling population-level studies. With sufficient signal-to-noise ratios, observations achieve spatial resolutions within a few meters, rivaling spacecraft images. This discussion highlights only key elements, deferring more extensive technique and result discussions to other works (Benner et al. 2015, and references within).

Planetary radar observations critically support small body scientific investigations and planetary defense.

NEAs detected with modest S/N ratios still provide valuable radar data, including astrometry, rotation constraints, radar scattering properties (radar cross section and radar albedo), and the polarization ratio. Radar albedo requires physical diameter estimates from other methods, such as brightness at visible wavelengths. Radar albedo indicates surface density and metallicity (e.g., Shepard et al. 2008), and the circular polarization ratio serves as the zeroth-order surface roughness gauge; a circular polarization ratio of zero suggests a smooth surface at the wavelength scale. Quantitative radar scattering property analysis can help us understand asteroid surface diversity in terms of materials and structure.

Targets with sufficiently high S/N ratios can be resolved into two-dimensional delay-Doppler images (Figure 2.3). With image sets, it is possible to determine the object's size, shape, and rotation state. Sufficiently large delay-Doppler image sets from an NEA enable shape model development (e.g., Naidu et al. 2020; Shepard et al. 2021).

Radar observations provide a direct way to distinguish binary and ternary near-Earth asteroids from single bodies, revealing that approximately 15% of the entire NEA population likely consists of binaries or ternary objects. Radar

¹The 1000th asteroid was detected on 2021 August 22, only a few months after the second workshop for this KISS study, <https://www.nasa.gov/solar-system/planetary-radar-observes-1000th-near-earth-asteroid-since-1968/>. A census of radar-detected NEAs and comets is maintained at <https://echo.jpl.nasa.gov/History/>.

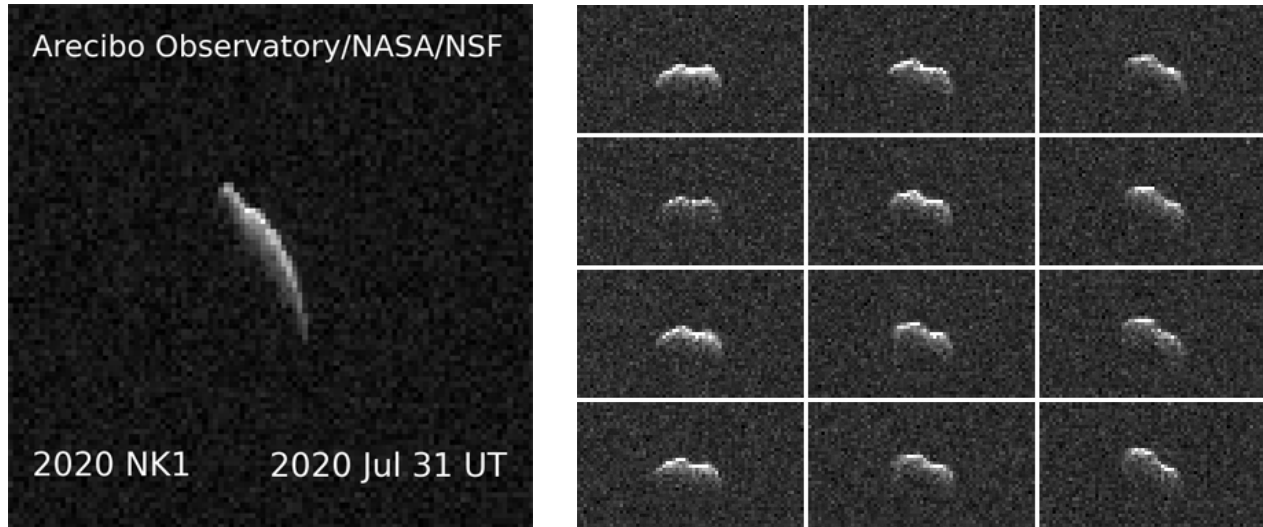


Figure 2.3: Near-Earth asteroid delay-Doppler image illustrations acquired during this KISS study. In both cases, the direction to Earth is toward the top of the page. (left) 2020 NK₁ was observed with the Arecibo Observatory on 2020 July 31, the last potentially-hazardous asteroid observed with the Arecibo Observatory. This asteroid measures approximately 1 km, which is rare for newly discovered near-Earth asteroids, as most asteroids this size are already known. The spatial resolution obtained is approximately 30 m per pixel. (Credit: Arecibo Observatory/NASA/NSF) (right) 2001 FO₃₂ observed with the Goldstone Solar System Radar and the Green Bank Telescope on 2021 March 21. The observations achieved approximately 35 m per pixel spatial resolution. Complementary radar observations used transmission from the 70 m antenna at the Deep Space Network's Canberra Deep Space Communication Complex in Australia with reception by the Commonwealth Scientific and Industrial Research Organisation's Australia Telescope Compact Array (ATCA). (Credit: NASA/JPL-Caltech and NSF/AUI/GBO)

observations enable comprehensive classification of binary asteroid size distributions, spin periods, and other physical characteristics such as masses and bulk densities, in addition to understanding their dynamical properties. Extended binary system tracking improves determinations of secondary orbits, system masses, and density, parameters otherwise constrained only through compositional inference or indirect suggestion from the Yarkovsky effect.

Objects in non-principal axis (NPA) rotation have rotation states that depend on moment of inertia ratios, which constrain the objects' interiors. Longer tracking durations would provide better constraints for such objects. More detailed studies of a larger fraction of the NEA population, and of key sub-populations such as binaries and NPA rotators, are needed to learn more about their general properties.

Recent studies examining asteroid physical properties show that radar scattering properties can be used to interpret target surface properties only through comparison with other similar targets. Surface material and surface roughness both affect radar scattering properties ambiguously, so comparing asteroids within the same taxonomic type (similar surface material) helps constrain the parameter space. Therefore, smaller spectral complexes need more asteroid observations to increase quantitative analysis reliability.

Next-generation planetary radar systems involve two key considerations. First, maximum power, specifically the equivalent isotropic radiated power (EIRP), determines the largest possible volume for NEA detection. Second, optimum wavelength or wavelengths must be determined. Shorter wavelengths produce higher antenna gain and, under equivalent conditions, a higher EIRP. However, they do not provide much penetration into an object. Conversely, at longer wavelengths, the EIRP may be lower, but the signal penetration depth can be much deeper. A sufficiently powerful, long-wavelength ground-based planetary radar could conduct NEA tomographic studies (Haynes et al. 2023), extending the tomographic study concept from the single case with comet 67P/Churyumov-Gerasimenko during the Rosetta mission (Kofman et al. 2015) to multiple NEAs.

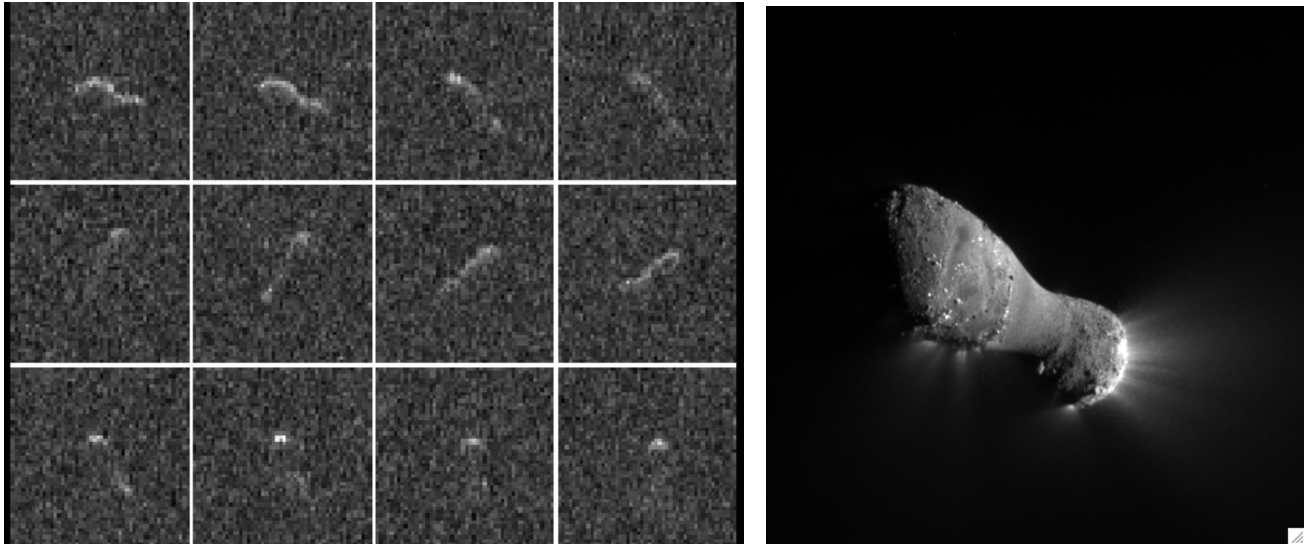


Figure 2.4: (*left*) Arecibo images of comet 103P/Hartley nucleus, acquired over two days, prior to the closest approach by the EPOXI spacecraft (2010 October 25 to 27, Harmon et al. 2011). (*right*) EPOXI image of comet 103P/Hartley, acquired from a distance of approximately 700 km on 2011 November 4 (A'Hearn et al. 2011). The comet nucleus' main body length is approximately 2 km, while the “neck” is approximately 0.4 km in diameter. (Credit: NAIC-Arecibo/Harmon-Nolan; NASA/JPL-Caltech/UMD)

Minimoons

A recently-identified NEA class consists of temporarily-captured orbiters, more colloquially known as minimoons. These NEAs are captured into metastable orbits, effectively bound to the Earth-Moon system (Jedicke et al. 2018). The minimoon count discovered has remained relatively small, smaller than some initial predictions suggested. However, the Vera C. Rubin Observatory’s Legacy Survey of Space and Time (LSST) may detect many more minimoons when operations begin. A sufficiently powerful planetary radar could then study these objects effectively, providing both scientific insights and practical advantages since minimoons may represent rapidly-accessible spacecraft targets.

2.2.2 Comets and Interstellar Objects

Planetary radars have observed 23 comets to date. Comets rarely approach close enough to Earth to result in sufficient S/N ratios, compared with NEAs. Nonetheless, the radar returns have provided valuable complementary data to ground-based visible- and near-infrared wavelength observations (Harmon et al. 1999, 2004) and spacecraft visits (Figure 2.4). Visible- and near-infrared wavelengths provide constraints on cometary nucleus surface properties, while radar observations can probe more deeply, potentially several meters deep.

Spectral, polarization, and Delay-Doppler cometary nucleus images suggest rough surfaces on the scales matching radar wavelengths (decimeters) and larger, blocky structures. Some planetary radar observations predating the Rosetta mission led to these conclusions, which found considerable support following the comet 67P/Churyumov-Gerasimenko nucleus imaging (hereafter 67P/C-G), which showed substantial horizontal and vertical nucleus structures (Thomas et al. 2015). Arecibo radar observations did not detect 67P/C-G, but even the upper limits could be combined with observations at other wavelengths to place constraints on the nucleus properties (Kamoun et al. 1998, 2014).

Radar reflections from cometary comae have indicated that comets can eject large grains with centimeter-scale sizes. The sample size is small, but the large grain mass loss rate can rival that estimated for gas and dust mass loss rates. The Arecibo observations of 73P/Schwassmann-Wachmann following its disintegration (Virkki et al. 2019) provided a particularly notable cometary coma study example.

A sufficiently powerful, long-wavelength ground-based planetary radar (Haynes et al. 2023) could conduct comet tomographic studies, expanding beyond the single Rosetta/CONSERT experiment case at comet 67P/C-G (Kofman et al. 2015).

To date, all comets with radar detections have been short-period comets. LSST operations should discover more long-period comets (Schwamb et al. 2018), including earlier identifications when they are more distant from the Sun. Long-period comets are thought to have much more pristine surfaces, compared with short-period comets. Radar detection targeting a long-period comet could provide valuable insights into nucleus structure, large grain production, or both.

ESA has selected the Comet Interceptor mission to combine this breakthrough in comet discoveries with a compact, agile spacecraft set that can perform close-up studies targeting a pristine comet likely entering the inner Solar System for the first time.² Radar data from a future system capable of rapid target acquisition would help characterize possible mission targets, enabling complementary international collaborations.

Interstellar Objects

The technical requirements for interstellar visitor radar observations are very similar to those for near-Earth asteroid characterization and comets. Current discovery rates for ‘Oumuamua-like objects reach approximately 0.5 yr^{-1} . The Vera Rubin Observatory and the potential Near-Earth Object Surveyor Mission (NEOSM) should increase this rate to a few per year within approximately 0.2 au of the Earth (Rice & Laughlin 2019; Eubanks et al. 2021). Most future ‘Oumuamua-like objects will likely have significantly higher velocities at infinity (v_∞), requiring streak-detection techniques for discovery and *rapid-response* (few-day) radar observations. Borisov-like objects will likely remain rare ($\sim 0.1 \text{ yr}^{-1}$, Eubanks et al. 2021). Both Borisov-like objects and long-period comets make excellent high-value radar targets for sensitive delay-Doppler imaging, especially with interferometric reception to break north-south ambiguity. For example, half the eight comets with extant radar or spacecraft flyby images exhibit bilobate structures (Harmon et al. 2011), suggesting similar multiplicity in both comet and minor planet populations.

2.2.3 Planetary Defense

Asteroids have hit the Earth, including notable impacts at Tunguska, Russia, in 1908 and Chelyabinsk, Russia, in 2013. Planetary radar NEA science measurements connect closely to planetary defense objectives (Figure 2.5), as radar measurements enable both orbit determinations and NEA characterization to assess impact hazards and inform potential mitigation strategies. The “National Preparedness Strategy for Near-Earth Object Hazards and Planetary Defense” (Planetary Defense Interagency Working Group 2023) identifies conducting and improving radar capabilities as one action toward enhanced NEA detection, tracking, and characterization.

The key measurements obtained by radar observations are astrometric—Doppler shift and delay (range). Crucially, these measurements are in a line-of-sight direction, orthogonal to the astrometric measurements obtained with visible- or infrared wavelength observations.

During planetary defense exercises (e.g., Chodas 2019), the extent to which radar observations can be used as part of the characterization of the (fictional) object of interest is often part of the scenario. Radar observations can determine additional asteroid properties such as surface features, size, and shape through received polarization ratios and delay-Doppler imaging, all contributing to impact hazard assessment and potential mitigation strategies (e.g., Levasseur-Regourd et al. 2006).

Even a single radar measurement during an asteroid’s discovery apparition dramatically reduces orbital uncertainties. Arecibo and Goldstone observations extended the accurate prediction window for NEA close approaches by an average factor of five (Giorgini et al. 2009). Radar astrometry across multiple apparitions can detect non-gravitational forces like the Yarkovsky effect, constraining object mass and other physical properties.

²<https://www.cometinterceptor.space>

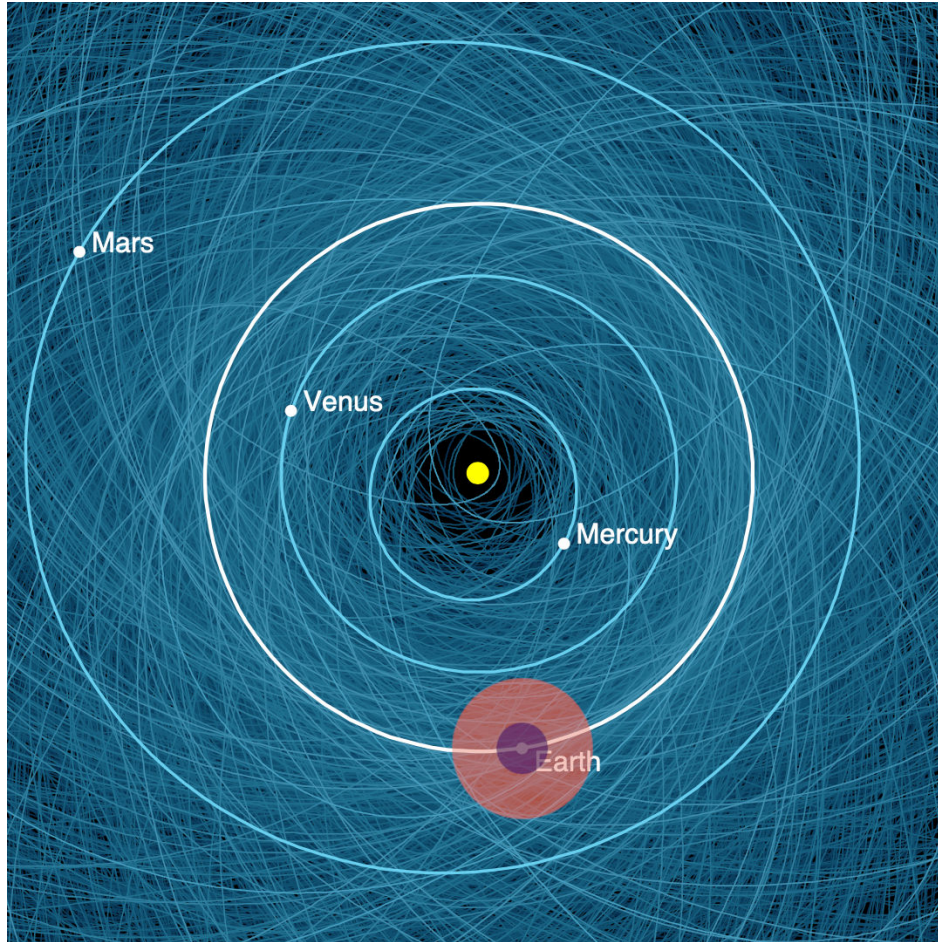


Figure 2.5: Orbits of potentially hazardous asteroids (PHAs), defined as asteroids with absolute magnitudes brighter than 22.0, corresponding to a diameter greater than about 140 m, that can come within 0.05 au of Earth's orbit. As of 2021 May 25, 2167 PHAs were known. The rings around Earth show the distances at which a relatively small PHA would be detectable within one hour ($S/N \geq 10$), with Arecibo and with capabilities comparable to that of the Next Generation Arecibo Telescope concept (in orange). This figure only shows a snapshot of the planetary positions (on 2021 July 1). Over time, as the planets and asteroids move around their orbits, every single one of these PHAs will eventually come close to Earth. (Credit: P. Chodas)

For planetary defense purposes, the smallest relevant targets are about 30 m in size (“Defending Planet Earth: Near-Earth-Object Surveys and Hazard Mitigation Strategies,” National Research Council 2010; “National Preparedness Strategy & Action Plan for Near-Earth Object Hazards and Planetary Defense,” Planetary Defense Interagency Working Group 2023). Most smaller objects, if on an impacting trajectory, would break apart in Earth’s atmosphere.

Two notable asteroids with planetary defense relevance for which radar observations have played significant roles are 99942 Apophis and 65803 Didymos-65803 Dimorphos I.

99942 Apophis

Initial Apophis orbit determinations indicated a series of close approaches (2029, 2036, 2068, ...), with a non-zero impact probability at each one. With a size of approximately 340 m, an Earth impact would have significant local to regional effects. Beginning in 2005, a series of radar astrometry measurements have contributed to successive impact risk eliminations. In 2005 and 2006, radar observations revealed a bias in some visible-wavelength astrometry and

made a 5σ correction in the Apophis orbit, moving the 2029 encounter prediction 4.4 Earth radii closer to Earth, but with no impact potential. These radar observations confirmed orbit predictions informed by Spacewatch precovery measurements that eliminated the 2029 impact potential. A subsequent impact potential in 2036 was eliminated by a combination of a long arc of visible-wavelength observations and radar observations in 2012–2013, with the latter providing Yarkovsky acceleration detection. The combination of visible-wavelength and radar observations in 2020–2021 removed yet another impacting keyhole in 2068.

Radar observations have played a significant role in revealing Apophis' size and shape and in confirming its spin state. Radar observations in 2012 and 2013 revealed an elongated, asymmetric object that is likely bi-lobate. The delay-Doppler images placed a lower bound on the long axis of 450 m and yielded an equivalent diameter of $340\text{ m} \pm 40\text{ m}$ (Brozović et al. 2018b).

Apophis will encounter Earth within 4.9 Earth radii from the surface in 2029. An object with its size approaching Earth this closely occurs about once in 6000 years. At the time of the closest approach, on April 13, 21:46 UTC, Apophis will be visible with the unaided eye, approximately as bright as the stars in the Little Dipper (the constellation Ursa Minor), and it will be moving rapidly across the sky. The best places to view this dramatic flyby will be northwest Africa and southwest Europe. The flyby's proximity is expected to significantly alter Apophis' orbit and spin state, although changes to its mass distribution or surface features are less likely. This rare event presents a planetary defense exercise and a major scientific opportunity.

65803 Didymos-65803 Didymos I Dimorphos and the Double Asteroid Redirection Test (DART)

NASA's Double Asteroid Redirection Test (DART) mission marked the first real-world attempt to deflect an asteroid. The goal was to test the kinetic impactor technique as a technology to alter an asteroid's orbit, i.e., impart momentum onto an asteroid by ramming a mass into it at high speed. The mission targeted Dimorphos, the secondary of Didymos, specifically because its binary nature allowed a single spacecraft to demonstrate the technique, with follow-up ground-based observations confirming the orbital shift of the secondary. Ground-based planetary radar, the key tool for discovering binary asteroids, was critical in mission planning and design. Additional mission design considerations included the required " ΔV ," the secondary's size, close Earth approaches, post-impact eclipse opportunities, and general system characterization (Rivkin et al. 2021; Rivkin & Cheng 2023). Ahead of DART's launch, Naidu et al. (2020) analyzed S- and X-band radar observations to map Didymos' 3D shape, spin state, scattering properties, and system bulk density, along with the detailed characterization of the secondary. After impact, radar confirmed the orbital change of Dimorphos with high precision (Naidu et al. 2024), providing the first indications that the DART mission successfully changed the orbital period by more than the required amount.

2.3 Main Belt Asteroids

2.3.1 Asteroid Families

The detection and characterization of asteroids with common origin (asteroid family's members) help us understand planetary formation and evolution in the Solar System. If one could identify and remove all the family asteroids from the Main Belt, the remaining population would be composed of the intact planetesimals, the properties of which, such as size-frequency distribution (e.g., Delbo' et al. 2017; Nesvorný et al. 2024), hold clues to Solar System formation and subsequent evolution. Starting with the pioneering work of Hirayama (1918), asteroid families traditionally have been identified by looking for clusters in proper orbital elements. (See Nesvorný et al. 2015 and Knežević 2016 for reviews.) Modern challenges include distinguishing small family members from the "background population" (the problem of interlopers) and identifying families older than 1 Gyr, for which the fragments' orbital elements have lost their initially tightly-packed clusters due to the Yarkovsky effect and resonance sculpting.

Physical properties such as albedo, spectral color, and reflectance spectra increasingly help break degeneracies and validate clustering results to address these issues. Masiero et al. (2015) reviewed these properties extensively.

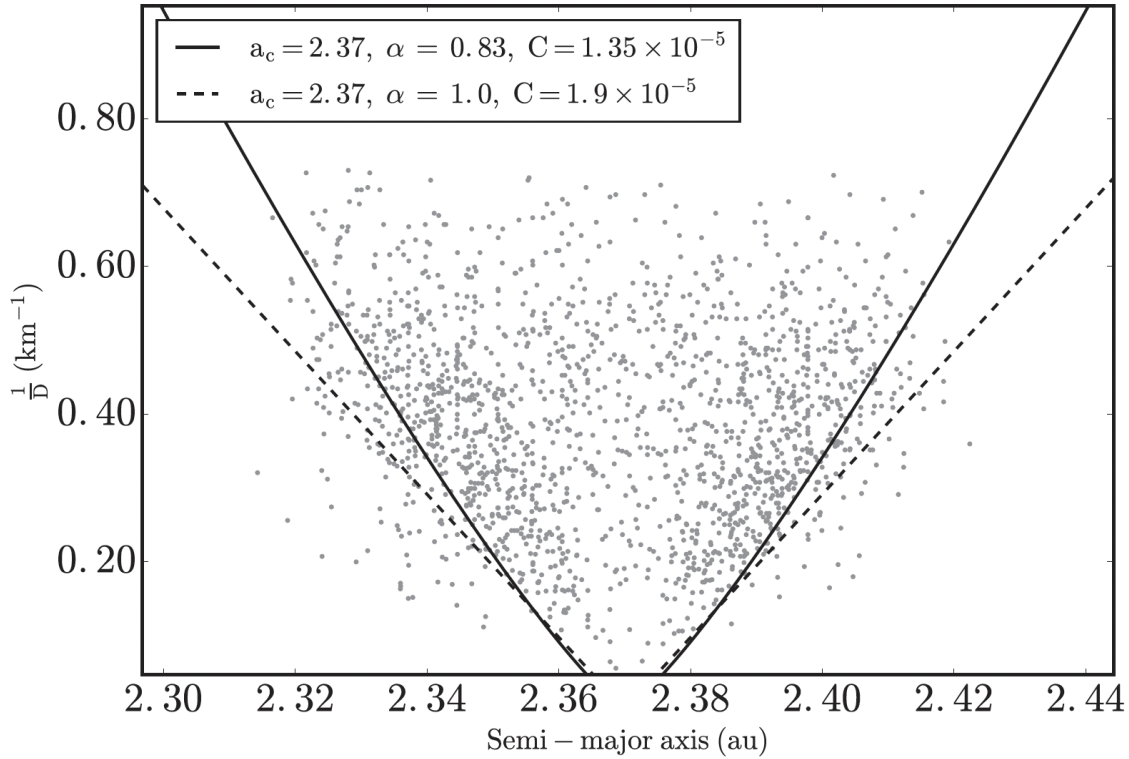


Figure 2.6: V-plot for the inner-Main Belt Erigone family in semi-major axis a and reciprocal diameter $1/D$ space. Lines representing the approximate outer V-shape border of the family are overplotted, assuming no size-dependence on thermal inertia (dashed line) and size-dependence on thermal inertia (solid line) using the V-shape approximation methods. Adapted from Bolin et al. (2017, 2018).

However, the physical property dataset still lags far behind the orbital dataset (Milani et al. 2014), though ongoing surveys are currently dedicated to closing this gap (e.g., the Primitive Asteroids Spectroscopic Survey, Pinilla-Alonso et al. 2017; Rizos et al. 2019). Improved radar surface property measurements (albedo, SC/OC, diameters) would be extremely valuable for confirming family membership through classical clustering methods or new approaches such as Yarkovsky V-shapes (e.g., Bolin et al. 2017) or machine learning (e.g., Carruba et al. 2019). This includes diagnosing variations between fragments within the same family to constrain parent body heterogeneities (a proxy for their interior structure) and examining the relationship between radar-inferred asteroid regolith properties and their family ages. The latter would provide information about regolith formation process timescales and thus provide context for meteorite formation.

Multi-wavelength observations (e.g., combining thermal infrared, millimeter-wavelength, and radar observations) are essential efforts to measure asteroid spins, shape models, and thermal inertia and improve current Yarkovsky effect models (Figure 2.6; see also Bolin et al. 2017, 2018) and asteroid family evolution. Multi-wavelength studies examining asteroid family member regolith and colors across varying ages may provide additional insights into space weathering processes on asteroid surfaces (Nesvorný et al. 2005).

2.3.2 Ice in the Main Belt

Answering the question of how much ice is in the Main Belt—and how it is distributed with heliocentric distance—is crucial for understanding the distribution of water in the early Solar System and its delivery to Earth. Lunine (2006) proposed that the snow line in the protoplanetary disk fell within the current Main Belt while Walsh et al. (2011) proposed that many of the current Main Belt asteroids formed farther out in the Solar System where water ice is

stable. Both meteorite studies and asteroid spectroscopy have demonstrated that water and aqueous alteration are widespread within the Main Belt (Brearley 2006; Takir & Emery 2012). Aqueous alteration surveys across the Main Belt rely on characteristic spectral absorptions in the visible- and near-infrared (De Prá et al. 2018; de Leon et al. 2019; De Prá et al. 2020a,b). However, such observations are only sensitive to asteroid surfaces, which have been subject to micrometeorite bombardment and space weathering for billions of years. How much water ice is buried under these regoliths, including how pure the ice is and how it is distributed with heliocentric distance, cannot be answered with visible to near-infrared wavelength observations except at recently fractured objects that expose their fresh interiors. Long-wavelength radar (70 cm, UHF band) probes beneath thick asteroid regolith, while ice produces highly radar-reflective signatures clearly distinguished from typical asteroid surface materials. The distinctive radar signature of ice has been used to deduce the presence of subsurface water ice on Mercury and the Galilean moons and to search for it on the Moon (e.g., Ostro & Shoemaker 1990; Campbell et al. 2003b; Black et al. 2010). A UHF-band radar system with sufficient power to detect reflections from icy asteroid subsurfaces (sizes around tens of kilometers, at geocentric distances around 2.2 au) could survey Main Belt asteroid subsurface ice content and produce potentially ground-breaking insights into ice distribution across the Main Belt and hence in the early Solar System.

2.3.3 Interior Structures

Radar observations could provide measurements allowing interior structure constraints for Main Belt asteroids, (Asphaug et al. 2002), which may help constrain the Main Belt's collisional history and potentially even early Solar System planetesimal formation (e.g., Tatsuuma et al. 2024). A next-generation radar system with sufficient power could obtain shape and size constraints through standard delay-Doppler imaging and shape modeling. Some fraction of imaged asteroids will be binary systems, allowing mass determinations. These observations can constrain bulk densities. Non-principal axis rotation objects could provide moment of inertia constraints, which would yield stringent interior structure constraints.

2.3.4 Active Asteroids

Historically, there has been a division between asteroids and comets. Among the properties distinguishing the two classes of small bodies, asteroids were defined as exhibiting no outgassing, while comets were distinguished by and often discovered as a result of significant outgassing, which is then responsible for the at-times significant tails that they exhibit. This distinction has become less clear over the past decade as a class of so-called “active asteroids” was discovered. Jewitt (2012) and Jewitt et al. (2015) have reviewed the observations and inferences about these objects. Active asteroids initially showed properties consistent with asteroids at discovery, but later revealed at least some properties, notably outgassing, consistent with comets. Recent impacts, excavating or uncovering subsurface volatiles, might explain some active asteroid fraction, but recent impacts could not explain all active asteroid properties.

No radar observations of an active asteroid exist to date, but acquiring such observations would provide insight into the processes occurring on active asteroids. Specific questions that could be addressed would include whether episodically active asteroid surfaces, such as (62412) 2000 SY₁₇₈ or (6478) Gault, are being resurfaced during active periods or how active asteroid surface properties compare with the larger asteroid population surface properties.

2.4 Outer Solar System: Satellites and Small Bodies

Both volatile and refractory material distributions on outer Solar System satellites are important tracers for their geological activities, habitabilities, and seasonal evolution. Radar observations have been key to tracing volatiles on Solar System surfaces because volatile deposits, and more generally different geological terrains, may have quite different dielectric properties and hence distinctive radar signatures.

2.4.1 Galilean Satellites

Europa, Ganymede, and Callisto are “icy” bodies, composed of rock and (water) ice mixtures. Early planetary radar observations provided crucial evidence supporting their icy natures (Campbell et al. 1977; Ostro & Pettengill 1978). All three bodies are differentiated to some extent, with at least a rocky mantle (and sometimes a metallic core) overlain by a water ocean and a thick icy crust. In contrast, Io, the innermost Galilean satellite, is a mostly rocky body with a metal core and no surface water ice. Instead, large surface areas are covered with sulfur dioxide ice, originally expelled by volcanic activity. Comprehensive reviews on these bodies are available in Burns & Matthews (1986), Bagenal et al. (2004), Pappalardo et al. (2009), and Lopes et al. (2023).

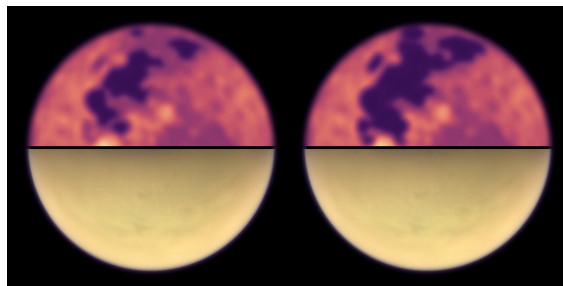
The important objective for the Galilean satellites is mapping the time-dependent volatile distribution on their surfaces, and for Io, lava as well. Surface volatile distribution changes on the icy Galilean satellites may result from diurnal or seasonal effects, or alternatively from volcanism or cryovolcanism. For Io, changes may arise from surface lava distribution variability (areal extent, fluid vs. solid, smooth [pahoehoe] vs. jagged [a’a]) resulting from magma in conduits rising to the surface during large eruptions.

These objectives would address the priority science questions, “How Have Diverse (Cryo)Volcanic Processes Shaped Solid Body Surfaces, Physically and Chemically?” and “Where and How Are Active Melt Generation, Outgassing and Plume/(Cryo)Volcanic Activity Taking Place, and What Melt and Gas Compositions Are Produced?” identified in *Origins, Worlds, and Life* (2022).

A specific and compelling example for Io would be observing eruption evolution at Loki Patera, a 200 km diameter horseshoe-shaped patera, which shows “brightening” events at infrared wavelengths about every 420–540 days (Rathbun et al. 2002; Rathbun & Spencer 2006; de Kleer & de Pater 2017; de Pater et al. 2017). Loki Patera has been proposed to be a lava lake, where brightenings are caused by crust foundering and breaking, leading to hot underlying magma exposure. An alternative hypothesis suggests it is the site for patera eruptions as seen at other Io locations, but with long-term periodicity. Multi-frequency radar measurements at high spatial resolution during eruption waxing and waning phases would help elucidate the process.

A lava lake would have different dielectric properties from surrounding regions. During the phase leading up to eruption, magma should rise (liquid closer to the surface) and crust founder (increase subsurface scattering component), while new hot lava is ejected onto the surface (increases scattering component). A regular eruption above a magma chamber may show magma rising to the surface in a narrow conduit, and lava flowing away from the eruption site.

The above example has been quite specific, but there are numerous locations on Io where eruption details are simply not known. Pele, the volcanic site at the red ring center, is another example. There may be differences between eruptions at equatorial-to-mid-latitudes and closer to the pole; alternatively, some eruptions may result in gaseous plumes, while others do not. Plume composition appears to vary across the disk, since SO₂ gas plume locations do not coincide with those containing the salts NaCl and KCl (de Pater et al. 2020).



Titan's methane lakes could be monitored for seasonal changes.

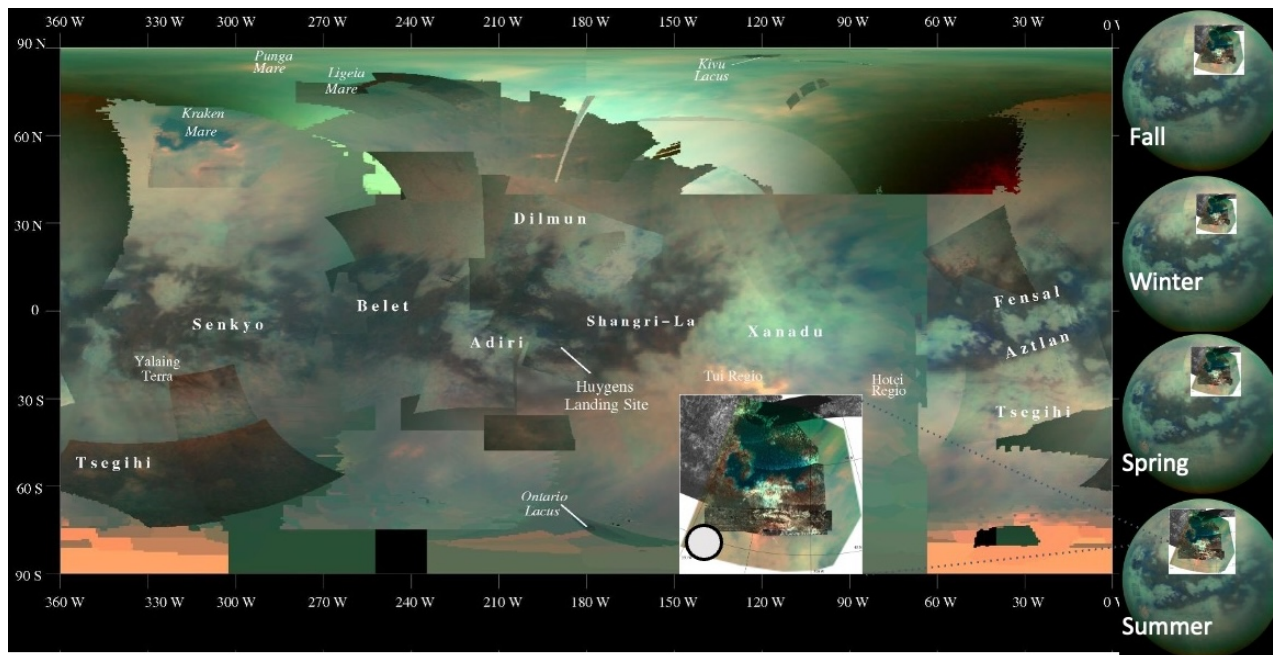


Figure 2.7: Illustration of Titan's surface, with the insets to the right suggesting how the extent of Titan's lakes could change with its seasons. (Credit: NASA/JPL-Caltech/Univ. of Arizona/B. Butler)

Icy satellite areas with cryovolcanism or recent outgassing, if present, would produce surface deposits that differ in radar scattering properties from surrounding terrain and may be variable in time, if activity is ongoing currently. Even without temporal variability, terrains with different geological origins (e.g., tectonics vs. impact craters vs. old terrain) on the icy Galilean satellites exhibit different passive radio emission signatures at frequencies below 1 GHz to higher than 100 GHz, which could be similarly identified by radar to contribute to our understanding regarding different terrain origins (as observed by ALMA and Juno's MWR; Brown et al. 2023; Zhang et al. 2023; Trumbo et al. 2018; de Kleer et al. 2021; Camarca et al. 2023).

2.4.2 Titan

Titan's surface temperature and pressure are near the triple point of methane, leading to a dynamic methanological cycle that includes storm systems, rain, and seasonal lakes. This property, combined with its dense (1.5 bar), chemically complex atmosphere, makes Titan a target of great interest from an astrobiological perspective. Photochemically-produced hydrocarbons in its atmosphere rain out into vast dune fields in its equatorial regions. The resultant surface terrain diversity on Titan leads to dielectric properties that differ greatly at the regional scale, and hence generate distinctive radar scattering signatures. Radar is particularly sensitive to surface liquid presence, and has been used in the past to detect specular glints from Titan's surface indicative of current or past liquids (Campbell et al. 2003b; Black et al. 2011; Hofgartner et al. 2020).

Titan's atmosphere is thought to host a single circulation cell that reverses as seasons change, with upwelling at the summer pole and downwelling at the winter pole. Convective storm activity is predicted towards the southern pole (Lora et al. 2015), and surface changes have been detected directly following methane precipitation events (Turtle et al. 2011), indicating a direct connection between seasonal storm activity and the filling of lakes and seas (Figure 2.7). However, Titan has not yet been observed in detail through its entire year, and so far has not behaved as predicted during northern summer (Lora et al. 2015), indicating that its climate system is not yet understood. Storm systems can be detected from Earth in the near-infrared, but the only way to detect Titan's lakes in the absence of a Saturn system orbiter is by detecting the distinctive radar reflection signatures.

Future radar observations would address the priority science question “Where and How Have Fluvial Processes Sculpted Landscapes?” identified in *Origins, Worlds, and Life* (2022) and related questions about Titan’s climate evolution. Such observations would provide important context for the detailed but localized studies to be performed by *in situ* missions such as *Dragonfly* (Barnes et al. 2021).

The specular glints previously detected in Arecibo and Green Bank observations were attributed originally to direct lake reflections on Titan, but the most recent comparison with *Cassini* imaging data disagrees. Hofgartner et al. (2020) suggests that radar is instead detecting “paleolakes” because the radar glint surface locations do not correspond to current lake locations. Such paleolakes appear as glints because of unique dielectric properties in the dry lakebed deposits, plus their high degree of smoothness. Under the paleolake hypothesis, these dry lakebed compositions may provide key information about Titan’s lake chemistry and climate history. However, other possible interpretations, including cryovolcanism and transient liquids, remain viable.

A key advantage of ground-based radar over spacecraft missions is the ability to observe changes on seasonal timescales, given Saturn’s 29-year orbital period. Any seasonal changes in geological terrain shape or extent—such as the equatorial dune fields, which may be affected by circulation direction—would also be detected provided the changes are at a sufficiently large spatial scale for radar detection and resolution. Titan’s lakes, dunes, and other terrains are a key aspect for understanding long-term volatile cycles and crustal processes. Earth-based radar can study these features far beyond the *Cassini* time horizon, and provide a global perspective to complement *in situ* studies from missions such as *Dragonfly*.

2.4.3 Other Satellites

We focus on the Galilean satellites and Titan as motivating cases in this report, but clear analogous value exists in planetary radar observations targeting Uranus’ satellites and Neptune’s moon Triton. Some Uranian moons (e.g., Ariel, Miranda) show evidence for past large-scale tectonic activity. The large-scale fracturing observed at visible wavelengths may produce distinctive radar scattering signatures, while regional variations in geological terrains (e.g., Triton’s so-called cantaloupe terrain) have different volatile contents that could be associated with different dielectric properties detectable with radar.

Similar priority science questions from *Origins, Worlds, and Life* (2022) apply to these bodies as for the Galilean satellites (§2.4.1), but the knowledge state for all of these bodies is considerably less and the discovery space wider, given that only a single fly-by has occurred, conducted by the Voyager 2 spacecraft.

2.4.4 Hildas, Trojans, and Centaurs

More powerful observational tools enable increasingly detailed investigations of smaller, more distant icy bodies. The Jupiter Trojans are co-orbital asteroids, orbiting near the Sun-Jupiter L4 or L5 points, and several will be visited by the Lucy mission. Hilda asteroids are a family on orbits interior to Jupiter, in a 3:2 resonance. Centaurs are a family of small bodies with orbits exterior to Jupiter that can show properties of both asteroids and comets.

Much of the focus on these objects has been their dynamics, but planetary radar observations would provide a means for addressing their characteristics beyond their reflected spectra, thereby contributing to one strategic research direction identified for addressing the science priority question “How Was the Inner Solar System Affected by Giant Planet Migration After the Gas Disk Dispersed?” in *Origins, Worlds, and Life* (2022). Planetary radar observations would enable measurements of their sizes, shapes, and spin states, and characterize their surfaces and near-surface structures for general population studies and a refined understanding of their accretion and evolution.

Near-surface scattering is particularly interesting for identifying the presence and distribution of any large volumes containing relatively pure water ice within several radar wavelengths from the surface, potentially underneath regolith or organic layers, which would indicate extensive ice-rock fractions. Such data would be strongly complementary to data just starting to emerge from *JWST*, which provides unprecedented information about the volatile contents

of distant icy body surfaces (e.g., Brown & Fraser 2023). The surface (*JWST*) and subsurface (radar) observations would collectively provide powerful insight into volatile accretion onto small bodies within the protoplanetary disk.

Radar observations might also detect larger satellites and ring systems, providing better orbital information and mass constraints. These planetary radar constraints on porosities, shapes, spins, and sizes would be combined with Wide-field Infrared Survey Explorer (WISE) observations (WISE, Grav et al. 2012b,a; Bauer et al. 2013), the *Herschel* Trans-Neptunian Objects (TNOs) Are Cool project (Müller et al. 2009), and current/forthcoming *JWST* observations (e.g., Müller et al. 2023) to obtain a more general view of this outer Solar System small body population.

2.5 Science Case Requirements

The science cases described above lead to a variety of requirements, which can be considered to be either instrumental (telescope) or “mission” requirements.

Anticipating the discussion of Chapter 3, eqn. (3.2) is reproduced here as it provides context for many of the telescope requirements. (Consequently, some of the elements of this discussion are repeated in that chapter.) The power from a radar transmission toward a target is determined by the radar equation,

$$P_{RX} = \frac{1}{4\pi} G_{RX} [P_{TX} G_{TX}] \lambda^2 \left[\frac{\sigma_{\text{radar}}}{(4\pi)^2 R^4} \right],$$

where G_{RX} is the gain of the receiving system, G_{TX} is the gain of the transmitting system, P_{TX} is the power transmitted by the transmitting system, λ is the wavelength of observation, σ_{radar} is the radar cross section (RCS), and R is the range or distance to the target. Also used commonly is the radar albedo η , which is related to the RCS as $\sigma_{\text{radar}} = \eta A_{\text{geom}}$, where A_{geom} is the geometric area intercepted by the radar beam. For reference, Figure 2.8 illustrates current capabilities, which provide a useful benchmark both to assess compliance with the set of science requirements and for consideration of any future facility. Figure 2.9 illustrates the potential reach of a future planetary radar system.

Wavelength (or Frequency)

The wavelength λ (or observing frequency ν) is driven by a variety of science considerations. In general, observing wavelength or frequency diversity is desired, as the extent to which surfaces reflect radar signals often is frequency-dependent, and wavelength or frequency diversity enables better surface (and near-subsurface property) characterization. Specifically, longer wavelengths or lower frequencies enable deeper subsurface penetration for many materials, enabling searches for subsurface ice, as in the Moon, Mercury, or asteroids, or asteroid interior characterization. Venus requires wavelengths longer than 10 cm or frequencies lower than 3 GHz to penetrate the atmosphere and obtain useful signal-to-noise ratios for returned signals. Scientific motivations also may have practical limitations regarding which wavelengths or frequencies can be used (§3.5.1).

Detectability of asteroid with $D = 140$ m

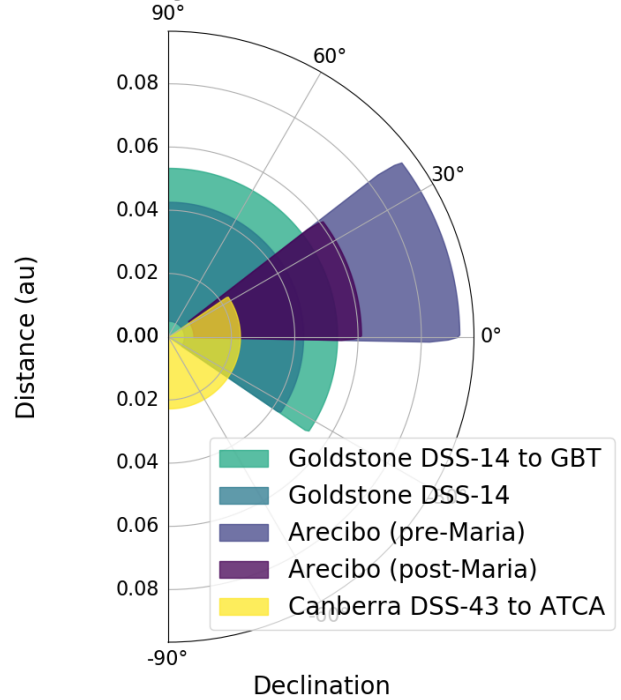


Figure 2.8: Distance from Earth at which a near-Earth asteroid with diameter 140 m (threshold to be considered potentially hazardous), rotation period 2.1 hr (spin barrier), and radar albedo 0.1 would be detectable ($S/N \geq 10$) within one hour, with past and present planetary radar facilities. (Credit: S. Marshall)

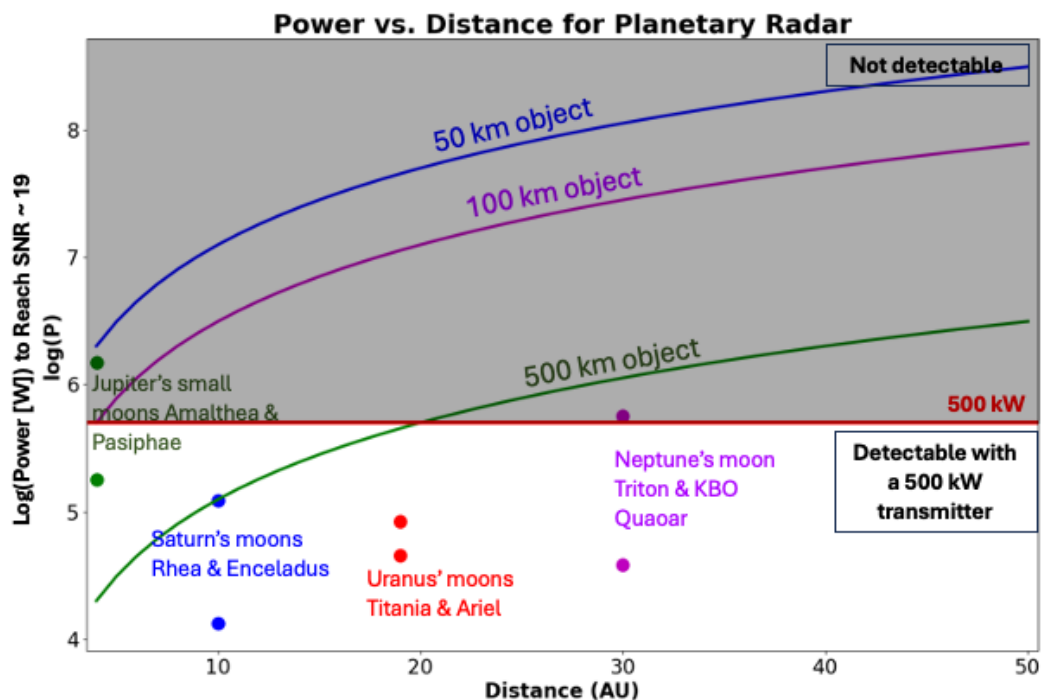
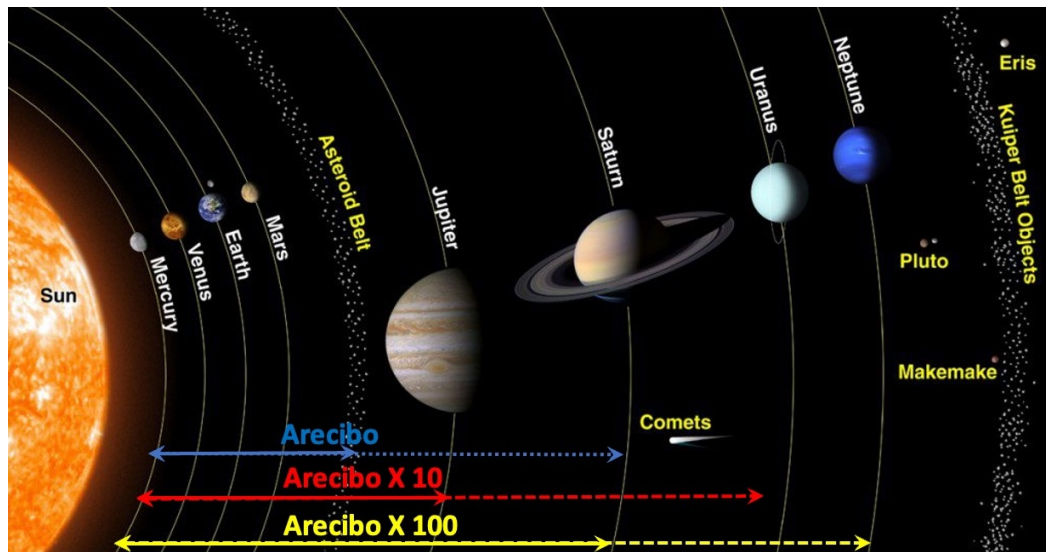


Figure 2.9: Two illustrations showing how a new planetary radar system could enable studies of a much larger number of Solar System bodies. (*top*) Illustrated is the extent of the Solar System that could be accessed with radar systems of increasing capabilities relative to that of the Arecibo Observatory. This figure assumes that the same system is used both to transmit and receive ($G_{TX} = G_{RX}$) and characterizes systems relative to the effective isotropic radiated power (EIRP) of Arecibo. The solid lines illustrate the ranges for which S/N ratios sufficient for delay-Doppler imaging would be achieved, while the dashed lines illustrate the ranges for which objects likely could be detected only with continuous wave (CW) transmissions. (*bottom*) Illustrated is the range in the outer Solar System that could be accessed with the GBT equipped with a 500 kW transmitter (Table 3.1) for objects of various diameters, and specific targets identified. (Credit: M. Brozovic, B. Butler, K. de Kleer)

Receiving System Gain

All other things being equal, a larger receiving system gain produces higher received powers and signal-to-noise ratios. Implementation considerations, however, suggest that receiving system gains have practical limitations. Current single dish antennas are at the scale at which larger antennas are not a viable approach for obtaining significant antenna gain improvements: No fully steerable single dish antenna significantly larger than the 100 m diameter Green Bank Telescope has been constructed since its completion in the early 2000s. (The 110 m-diameter Qitai radio telescope [QTT, Wang et al. 2023] may have begun construction, but its gain would be no more than about 20% larger than that of the GBT.)

Transmitting System

The transmitting system gain and power are often combined into a quantity known as the *equivalent isotropic radiated power*, $\text{EIRP} \equiv P_{\text{TX}} G_{\text{TX}}$. All other things being equal, a larger EIRP will produce higher received powers and higher signal-to-noise gains. For reference, the largest EIRP for a planetary radar system was 18 TW (Arecibo Observatory, Table 3.1).

Spectral Resolution

High spectral resolution, notionally a quasi-monochromatic signal, is required for the most basic detection experiments. A quasi-monochromatic signal can be used simply to detect a target, such as an asteroid, and for asteroid observations, the Doppler shift can be used to improve orbit determination. Measuring Venus' spin also benefits from a quasi-monochromatic signal.

Observing Bandwidth

The observing bandwidth $\Delta\nu$ determines the range of measurable Doppler shifts. Larger observing bandwidths both ensure that sufficient Doppler shift ranges can be obtained for orbit determination and enable improved delay-Doppler imaging. Sufficient observing bandwidths are required in some cases, e.g., Mercury, to ensure no imaging ambiguities.

Temporal Resolution

High temporal resolution δt is required to obtain high equivalent spatial resolution on a target. In general, spatial resolution is given by $c\delta t/2$, where c is the speed of light and the factor of 2 accounts for the time to travel to the target and back. Observations of Venus require time resolutions of $1\ \mu\text{s}$ to obtain 150 m spatial resolution; higher time resolutions ($< 1\ \mu\text{s}$) would be desirable for finer spatial resolutions.

Polarization

Full polarization on the receiving system is required for characterizing reflecting surfaces. In general, properties such as composition and “roughness,” or small-scale surface feature distribution, produce different polarization signatures.

System Reliability

High system reliability is required to ensure that the system can conduct observations when needed. Venus and outer Solar System body observations are either easier or, given historical system EIRPs, only possible when these targets are at their closest distances or minimum ranges. Near-Earth asteroid observations are either enhanced or only possible when they are at minimum distances, which can only be for short durations (a few days).

Improved Operations

Planetary radar systems with more streamlined operations would enhance or even enable increased science return. Survey and follow-up observations at visible- and near-infrared wavelengths involve substantial automation. From a radar perspective, target selection and scheduling, system configuration or “setup,” and subsequent data processing are all elements that would benefit from increased automation. Particularly for newly discovered near-Earth asteroid observations (targets of opportunity), more automated target selection and scheduling, and more automated system configuration could enable larger numbers to be observed.

Full Sky Coverage

Radar facilities in both northern and southern hemispheres would enable near-Earth asteroid tracking regardless of orbital properties (particularly orbital inclination) or arrival direction. Capabilities in both hemispheres also would enhance near-Earth asteroid orbit determinations by providing larger sky arcs.



3. Technical Concepts and Challenges

3.1 Summary of Current Capabilities

The ground-based planetary radar infrastructure (Figures 2.8 and 3.1, Table 3.1) can observe all terrestrial planets, the larger Main Belt Asteroids, the largest moons of Jupiter and Saturn, and near-Earth asteroids (NEAs) at distances of order 0.1 au, with typical NEAs being several hundred meters in diameter. Smaller NEAs can be observed at smaller distances, with objects of order 10 m and smaller having been observed at distances less than 1 lunar distance.

Table 3.1: Planetary Radar Infrastructure

System	Antenna	Transmitter Power	Transmit Frequency / Wavelength	Gain	EIRP
<i>Arecibo Observatory</i>	<i>305 m diameter</i>	<i>900 kW</i>	<i>2.38 GHz 12.6 cm</i>	<i>73.0 dBi</i>	<i>18 TW</i>
Goldstone Solar System Radar	70 m diameter	450 kW	8.56 GHz 3.5 cm	73.7 dBi	11 TW
Southern Hemisphere	70 m diameter transmit +50 m equivalent receive	80 kW	7.19 GHz 4.2 cm	72.5 dBi	1.4 TW
Deep Space Station-13 (Goldstone)	34 m diameter	80 kW	7.19 GHz 4.2 cm	67.0 dBi	0.4 TW
Green Bank Telescope ^a	100 m diameter	...	8.56 GHz 3.5 cm	77.9 dBi	...
		500 kW	13.7 GHz 2.2 cm	80.9 dBi	62 TW

^aThe GBT is not outfitted with a transmitter currently, though there is a concept for doing so (§3.2.2). Shown are its properties for both bistatic reception with existing facilities and with the concept for a future transmitter. The Arecibo Observatory is listed in italic font because, although it collapsed during the course of this study, data collected from it continue to prove valuable for a variety of studies.

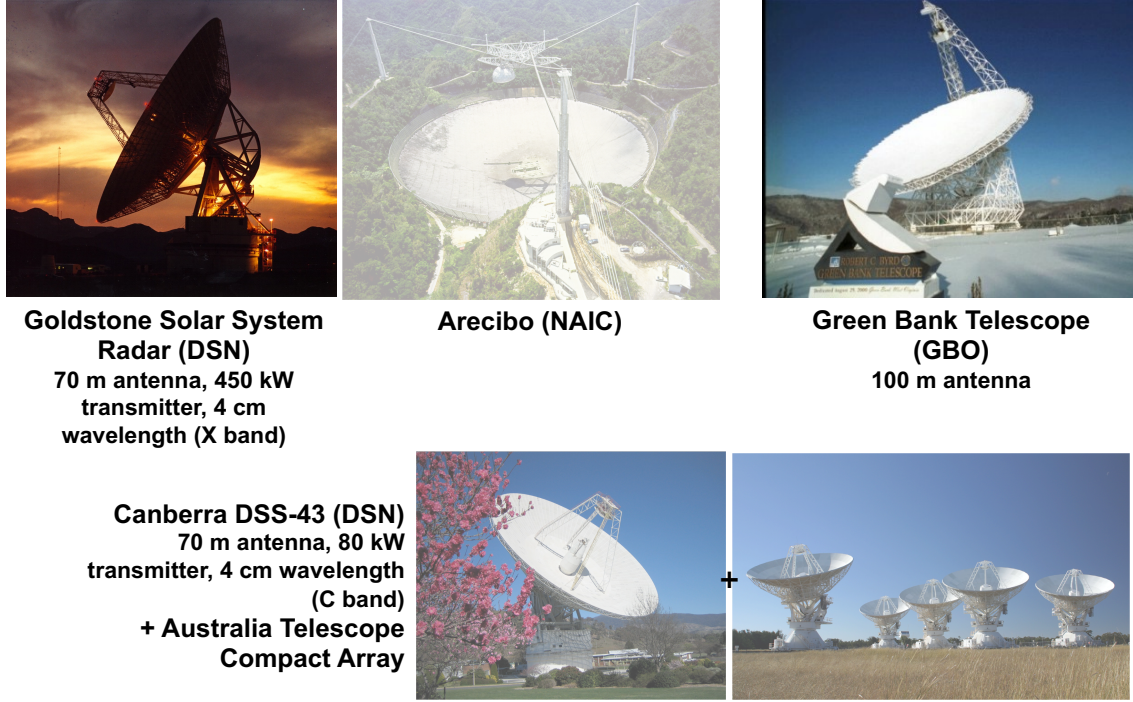


Figure 3.1: The international planetary radar infrastructure has enabled a variety of discoveries about all terrestrial planets, the largest moons, and near-Earth asteroids. Not shown are the Very Large Array (VLA) and the Very Long Baseline Array (VLBA), both of which have been used on occasion to receive transmissions from either Arecibo or the Goldstone Radar, nor Deep Space Station-13 (DSS-13), the research and development antenna within the Deep Space Network, which is used occasionally to transmit toward very close approaching near-Earth asteroids. While capable, particularly following the collapse of Arecibo, there are multiple aspects of this infrastructure that are fragile, warranting consideration of new capabilities. (Credit: NASA/JPL-Caltech; Univ. Central Florida/NSF; NRAO/AUI/NSF; CSIRO)

With its high gain and large transmit power, **Arecibo** was able to detect targets at the largest distances. However, Arecibo had a limited declination range and could observe only approximately 30% of the sky (centered approximately on a declination of $+18^\circ$). By contrast, the Goldstone Solar System Radar (**GSSR**), either monostatically or bistatically with the Robert C. Byrd Green Bank Telescope (**GBT**), can observe approximately 75% of the sky. Despite Arecibo's limited sky coverage, due to its transmit power and sensitivity, Naidu et al. (2016) showed that in a typical year, Arecibo could observe about twice as many NEAs as Goldstone could. Naidu et al. (2016) provides further technical details and comparisons between the various facilities, but, notably, most of this observational capability is based in the United States.

The vast majority of planetary radar observations involve unresolved targets. The signal-to-noise ratio obtained at a receiving antenna, from a radar waveform transmitted by a transmitting antenna, is

$$S/N = \frac{P_{RX}}{\Delta P_N} \sqrt{\Delta \nu \Delta t}, \quad (3.1)$$

where P_{RX} is the power received by the receiving antenna, ΔP_N is the noise in the receiving system at the receiving antenna, and $\Delta\nu\Delta t$ is the bandwidth-time product for the observations. In turn, the received power is determined by the radar equation,

$$P_{RX} = \frac{1}{4\pi} G_{RX} [P_{TX} G_{TX}] \lambda^2 \left[\frac{\sigma_{\text{radar}}}{(4\pi)^2 R^4} \right], \quad (3.2)$$

where G_{RX} is the antenna gain of the receiving antenna, G_{TX} is the antenna gain of the transmitting antenna, P_{TX} is the power transmitted by the transmitting antenna, λ is the wavelength of observation, σ_{radar} is the radar cross section (RCS), and R is the range or distance to the target. Also used commonly is the radar albedo η , which is related to the RCS as $\sigma_{\text{radar}} = \eta A_{\text{geom}}$, where A_{geom} is the geometric area intercepted by the radar beam. The notable factor of R^{-4} in the radar equation can be considered to be the consequence of Huygen's Principle—the transmitted signal suffers an R^{-2} loss by the inverse-square law in travelling to the target, the illuminated surface of the target then reradiates this signal, which suffers an additional factor of R^{-2} loss upon its return to the receiving antenna. Clearly, the radar equation assumes that the range or distance to the target from both the transmitting and receiving antennas is approximately the same, an assumption that is revisited in §3.4.

We now consider the various factors in eqns. (3.1) and (3.2), with a focus on those terms that are available for optimization or under the control of the observer. Notably, the factor $\sigma_{\text{radar}}/R^4$ contains terms that are target properties and not under observer control. Given the scientific requirements (§2.5), the KISS workshop focused on technologies that would increase transmit gain, receive gain, or both; increase transmitter power; improve the reliability of a planetary radar system; or achieve all of the above.

Noise Power

The noise power in the receiving system is $\Delta P_N = k_B T_{\text{sys}} \Delta\nu$, where k_B is Boltzmann's constant, the system temperature is T_{sys} , and the receiver bandwidth is $\Delta\nu$. These factors would seem to be under the observer's control. However, in practice, a well-designed system will use cryogenic receivers from which the noise contribution approaches fundamental limits. A typical value at the relevant frequencies is $T_{\text{sys}} \approx 25\text{ K}$. Similarly, optimized performance is obtained when the receiver bandwidth $\Delta\nu$ is well-matched to the *Doppler bandwidth* of the target, a topic to which we return below. In practice, modern receiving systems can obtain values of $\Delta\nu$ that are comparable to or higher resolution than the Doppler bandwidth of the target.

Antenna Diameter

For an antenna of diameter D with aperture efficiency ε operating at a wavelength λ , the antenna gain is $G = 4\pi A_{\text{eff}}/\lambda^2$, where the effective aperture is $A_{\text{eff}} = \varepsilon\pi(D/2)^2$. Importantly, current single-dish antennas are already at a scale at which building larger antennas is not a viable approach to achieving substantial improvements in gain. No fully steerable single-dish antenna significantly larger than the GBT has been constructed since its completion in the early 2000s. The Five-hundred-meter Aperture Spherical radio Telescope (FAST, Nan et al. 2017) has an even larger diameter than Arecibo, with the potential for higher gain. However, like Arecibo, it is constructed in a karst valley and can access only a limited region of the sky, albeit a larger fraction than Arecibo could. Consequently, if equipped with a radar system, FAST would not, on its own, meet a key science requirement. At the time of writing, we are unaware of any plans to equip FAST with a transmitter for use as a radar system.

Configuration

Radar experiments are conducted in both *monostatic* and *bistatic* configurations.

Monostatic: The same antenna is used both to transmit and receive, $G_{TX} = G_{RX}$. A prime benefit of monostatic experiments is simpler logistics; observations at only a single antenna have to be scheduled as opposed to coordinating observations at two antennas.

Bistatic: Different antennas are used for transmitting and receiving. Though potentially more challenging from scheduling perspectives, the observations are easier at each antenna, which either transmits or receives instead of switching between the two.

The mechanisms for switching between transmit and receive modes typically limit whether a monostatic experiment is possible. When the switching mechanism takes longer than the round-trip light travel time to the target, switching between transmit and receive is not possible. Historically, switching times at both Arecibo and the GSSR have exceeded 1 s, meaning that observations of objects closer than the Moon have required bistatic observations, a limitation that has affected some planetary defense observations (Reddy et al. 2024). At the GSSR, a switching system enabling switching times of approximately 1 s was installed in 2024 March.

Receiving Bandwidth

The optimum receiving bandwidth in the bandwidth–time product of eqn. (3.1) matches the Doppler bandwidth of the target, $\Delta\nu \propto d/(\lambda P)$ for an object with a diameter d and rotational period P . Modern systems can obtain bandwidths of 1 Hz or better, allowing the received signal to match the Doppler bandwidth well.

Integration Time

For monostatic observations, the integration time in the bandwidth–time product of eqn. (3.1) cannot exceed the round-trip light travel time to the target.

Effective Isotropic Radiated Power (EIRP)

A common metric for the performance of a radar system, particularly applicable for bistatic experiments, is the *effective isotropic radiated power* $\text{EIRP} = G_{\text{TX}}P_{\text{TX}}$. We use the EIRP of systems as a metric (Table 3.1); alternate formulations parameterize systems by $\text{EIRP}/\sqrt{\Delta\nu}$ or become more applicable for monostatic experiments.

Wavelength Diversity

Wavelength diversity is desirable from a scientific perspective (§2.5), but a system capable of receiving *and* transmitting at multiple wavelengths, either simultaneously or in rapid sequence, has received little investigation. As discussed in §3.5.1, regulatory considerations affect the wavelengths or frequencies at which a system can transmit. Further, while radio astronomy systems routinely observe over octave bandwidths, and multi-octave bandwidth systems have been demonstrated (e.g., Kooi et al. 2023), little research has examined how to implement transmitting systems across a range of wavelengths at the high power levels required for planetary radar applications.

3.1.1 Speckle Analysis

When illuminated with a continuous-wave (CW) transmission, the radar return from a target object forms a spherical pattern of regions of constructive and destructive interference called *radar speckles*. The speckles rotate with the target. Conventional CW observations average over many speckles as they pass across a receiving station. Radar speckle tracking, by contrast, measures the time lags of a series of radar speckles as they pass over two or more receive stations to determine a target’s spin state (Kholin 1992).

For objects with known spin states such as Mercury, Venus, and the Galilean satellites, speckle tracking can use very widely separated antennas and provide precise spin measurements that constrain models of the interiors of bodies and reveal changes due to tidal torques or atmospheric interactions (Margot et al. 2007; Holin 2010). For objects with unknown spin states, speckle tracking requires more closely spaced antennas, but it can provide unique spin state information when delay-Doppler radar images appear ambiguous (Busch et al. 2010).

With the current infrastructure, signal-to-noise limitations restrict speckle tracking to the largest few radar targets in the Solar System and to small NEAs making very close Earth flybys.

3.1.2 Radar Interferometry

Returning to an initial assumption underlying eqn. (3.1), some cases exist in which the target is angularly resolved. The terrestrial planets have angular diameters of tens of arcseconds, while the Galilean satellites and Saturn's moon Titan have angular diameters of approximately $1''$. Using a fiducial observing wavelength of 3.5 cm (8.56 GHz), a radio interferometer with the relatively modest scale of 10 km would obtain an angular resolution of approximately $1''$.

The *flux density* received by a radio interferometer is

$$S_v = \frac{P_{TX} G_{TX} \eta}{(4\pi)^2 \Delta \nu R^2} \Omega, \quad (3.3)$$

where many of the quantities are as in eqns. (3.1) and (3.2), and η is the radar reflectivity and Ω is the solid angle subtended by the target. (If the target is unresolved, then $\Omega = \pi d^2 / R^2$, where d is the target's diameter, and eqn. [3.2] is recovered.) In addition to the scientific value of being able to map the radar reflectivity as a function of (angular) position on the target, and thereby improve inferences about its properties, eqn. (3.3) shows that, if the target can be resolved angularly, the R^{-4} dependence in the radar equation becomes a much less severe R^{-2} dependence.

Historically, the VLA has received signals for bistatic radar experiments involving a number of objects, including Mercury, Mars, and icy outer planet satellites (Muhleman et al. 1991; Butler et al. 1993; Harcke 2005). More recently, a lack of improvements in transmitter capabilities, the availability of missions with dedicated radar instruments, and the focus on near-Earth asteroids have limited such interferometric observations. However, a radar array (§3.3) could revitalize this technique, particularly for icy outer planet satellites (potential “ocean worlds”) that may receive only limited visits from spacecraft.

3.2 Future Capability: Ground-Based Single Antenna Radar Systems

3.2.1 Overview

The next generation of radar systems can advance quickly by using existing infrastructure to develop an advanced radar system. A radar system deployed on a large single dish telescope such as the 100 m GBT (Figure 3.1), operating in either monostatic or bistatic mode, could significantly advance planetary science research. Additionally, single dish telescopes are the ideal platform for testing new technologies.

3.2.2 The Path Forward

A concept of a high-power radar system for the GBT was introduced by Bonsall et al. (2019), who envisioned outfitting the antenna with an approximately 500 kW transmitter operating at 35 GHz ($\lambda 8.6$ mm). Such a system would complement the GSSR's wavelength and achieve a much higher EIRP because of the larger antenna gain.

Wilkinson et al. (2022) demonstrated the GBT's planetary radar potential by deploying a 650 W system operating at 13.9 GHz (Ku band, $\lambda 2.2$ cm) in bistatic mode, with reception at the Very Long Baseline Array (VLBA). This demonstration produced radar returns from the Moon and, fortuitously, from the near-Earth asteroid (231937) 2001 FO₃₂ during a close approach.

Since the KISS workshop, the design of a high-power transmitter for the GBT, based on experience from the earlier demonstration, has been developed. Envisioned is a system with a comparable power to the earlier concepts (i.e., ~ 500 kW), but operating at a nominal frequency of 13.7 GHz (Ku band), similar to the demonstration system, rather than at 35 GHz (Ka band) as in the initial concept.

To date, most GBT radar planning has focused on transmitter hardware because the GBT lacks a transmitter. To meet all science requirements (§2.5), a parallel effort on operations likely would be required. Examples of the

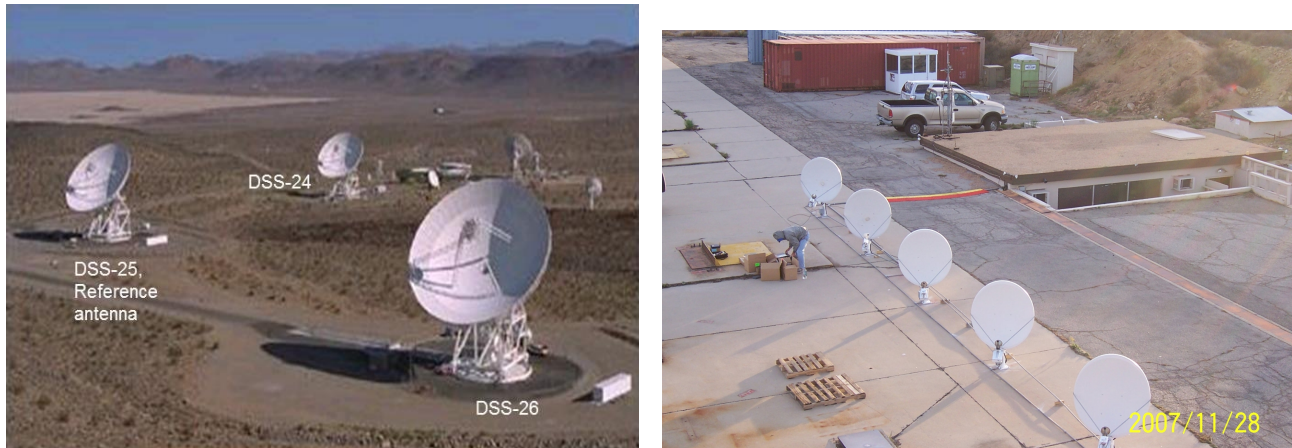


Figure 3.2: The capability to phase transmitting antennas coherently, as would be required for a future, operational planetary radar array, has been demonstrated with antennas of the Deep Space Network (*left*), the Loop Canyon Array (*right*), and the Deep Space Advanced Radar Capability (DARC, *not shown*). (Credit: NASA/JPL-Caltech; California Institute of Technology, L. D’Addario)

operational improvements that likely would be required include expanding the GBT’s current scheduling system to enable rapid responses to newly discovered near-Earth asteroids and developing or adapting existing radar processing software to obtain the desired scientific data products.

If a high-power GBT transmitter is deployed and operated successfully, future developments could include expanding the set of operating frequencies to include UHF band (70 cm) or S band (13 cm). These additional transmitters would provide the desired wavelength diversity (§2.5) to probe the surface and near-subsurface properties of Solar System bodies and complement the current Goldstone capabilities. Developing the next-generation Very Large Array (ngVLA, Brozović et al. 2018a) as a receiver for a high-power GBT transmitter would greatly increase radar system sensitivity compared with using the VLBA to receive.

3.3 Future Capability: Ground-Based Radar Array

Phased arrays are standard in terrestrial radar applications, and interferometric (“receive-only”) arrays are well-developed for radio astronomical telescopes, with Sir Martin Ryle sharing the 1974 Nobel Prize in Physics for developing aperture synthesis techniques for radio astronomical arrays. Beyond their use as receiving elements in bistatic radar experiments (§3.1.2), the principle of *reciprocity* suggests that arrays of antennas, with each antenna equipped with a transmitter, can operate as transmitting elements in either monostatic or bistatic radar experiments.

The expected performance of a transmitting radar array is well developed and has been demonstrated with multiple test arrays (Figure 3.2 Vilnrotter et al. 2006; D’Addario 2008; Vilnrotter et al. 2009; D’Addario et al. 2009; Vilnrotter et al. 2010a,b, 2011; Vilnrotter et al. 2023). For an array of N identical antennas, the EIRP scales as N^2 , a relationship that offers two potential benefits. First, each antenna’s transmitter can operate at much lower power than has been used traditionally for single antennas (hundreds of kilowatts), improving transmitter reliability (§3.5.2). Second, much like receiving arrays, a transmitting radar array would degrade gracefully.

Tests reported in the references above include transmissions to the Mars Global Surveyor and the Extrasolar Planet Observation and Deep Impact Extended Investigation (EPOXI) spacecraft, which confirmed the N^2 scaling for a limited number of antennas (Figure 3.3). Additional tests toward Mercury, Venus, and asteroids demonstrated the capability to conduct planetary radar observations.

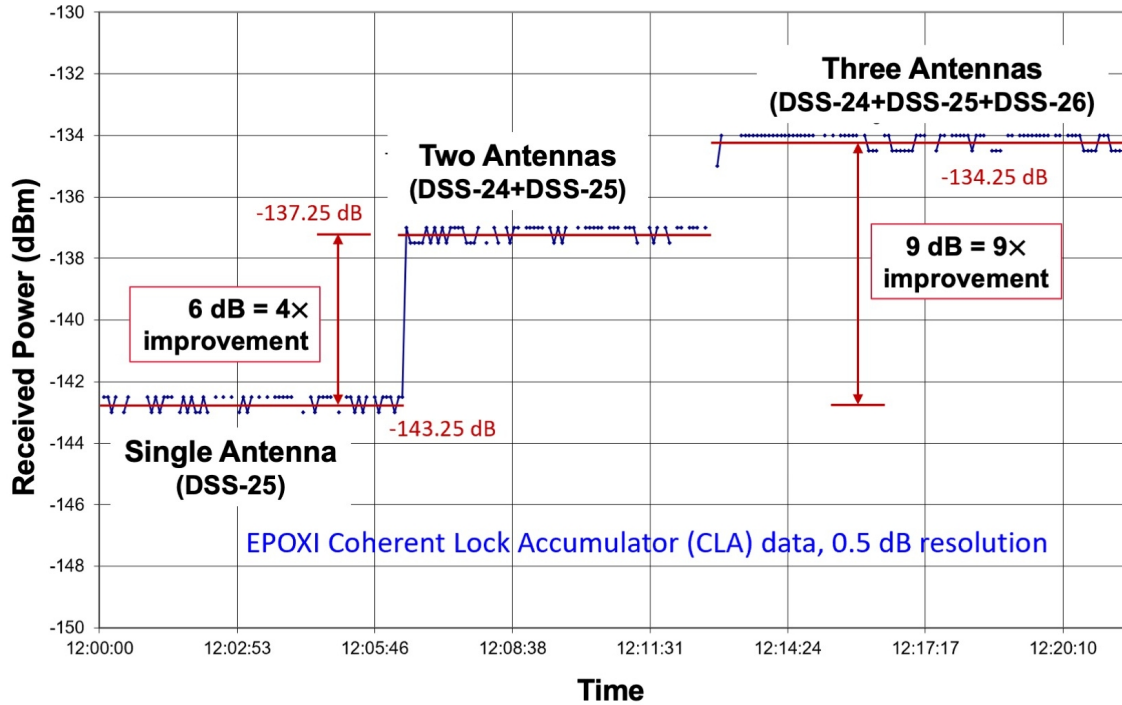


Figure 3.3: Demonstration of the expected N^2 improvement in equivalent isotropic radiated power (EIRP) for a transmitting radar array composed of three Deep Space Network antennas. (Adapted from Vilnrotter et al. 2009)

As a motivational example, an array composed of 45 antennas, each 18 m in diameter and equipped with a 50 kW transmitter and operating at 8.56 GHz, could have a projected EIRP more than 10 times that of Arecibo (Table 3.1). The loss of a few antennas from such an array might reduce its EIRP by about 10%, whereas the loss of a single klystron from either Arecibo or the GSSR can and has reduced their EIRPs by 50%. In contrast, obtaining significant improvements in EIRP from single-dish antennas involves multiple technical and engineering challenges (§3.1).

3.3.1 Calibration

A critical element of a radar array is phasing, as in a radio astronomical array. The requirement is that the electric fields from the individual antennas add coherently in the far field of the array. In principle, two approaches can be used to meet this requirement. One approach is to use a centralized radar waveform generator that produces a signal to be transmitted, with suitable delays injected into the signal path to account for the different path lengths to the individual antennas and the direction of the target in the sky. The alternate approach is to have radar waveform generators at each antenna, synchronized to a common reference. In either approach, delays to each antenna must be measured, and any temporal changes (e.g., from temperature-driven variations in electrical path length) must be monitored and compensated.

Calibration techniques using a *reference emitter* are mature for radio astronomical (receive-only) arrays. For a radar array, round-trip phase measurements could monitor the delays to each antenna. However, measuring the phase contribution of the feed or horn at the antenna is difficult, *and* the lines of sight from the different antennas through the Earth's atmosphere can have differential delays.

For a transmitting array, these considerations have led to the concept of a *reference receiver*. Scenarios tested include using a distant receiver or the Moon as a target (D'Addario 2008; Vilnrotter et al. 2010b). Tests show that, once calibrated, systems can remain stable for hours to days (D'Addario et al. 2009). For a future operational system, a receiver in geosynchronous orbit (GEO) has also been proposed.

3.3.2 Manufacturability

While DSN Complex antennas can and have been used to demonstrate aspects of a radar array, their use is unlikely to be a suitable long-term approach. The DSN's primary function is spacecraft telecommunications. While its mission could be expanded to include a more prominent role for planetary radar, in order to meet the requirements for both spacecraft telecommunications and planetary radar, additional antennas would be required. Therefore, consideration of a separate planetary radar array or arrays (for longitudinal coverage, §3.5.4) is warranted.

Multiple cost models have been developed for a planetary radar array. While they may differ in assumptions, a common feature is antenna diameters in the range of approximately 5 m to 20 m, smaller than those of the large single-dish antennas used previously for both radio astronomical and DSN antennas. The primary factor motivating smaller diameters is decreasing cost of the electronics (Schilizzi et al. 2007), which shifts the balance between the total cost of the antennas versus the total cost of the associated electronics toward an optimum at smaller diameters.

A consequence of adopting smaller diameter antennas is that more are required to achieve sufficient EIRP. Various estimates indicate that at least tens of antennas will be required, with an approximately equal number of transmitting and receiving systems. Arrays of this scale exist in radio astronomy, most notably the Karoo Array Telescope (MeerKAT) array in South Africa (Jonas & MeerKAT Team 2016), with 64 antennas each of 13.5 m diameter, and the Deep Synoptic Array (Sherman et al. 2023) in California, with 63 antennas each of 5 m diameter. An element of producing an operational planetary radar array will be to assure supply chains for all sub-systems, including transmitters (§3.5.2).

3.4 Space-Based Concepts

Space-based radar technology makes it possible to study certain targets and phenomena that remain inaccessible to ground-based radar, such as

- Bodies in the outer Solar System, such as satellites of Saturn or Uranus, and trans-Neptunian objects;
- Situations requiring high spatial and/or temporal resolution, such as time-resolved study of Titan's lakes, or for which the north/south ambiguity would otherwise present a problem;
- Use of frequencies blocked by Earth's atmosphere or by regulatory constraints; or
- In the more distant future, applications requiring high directivity, with constellations of interferometric spacecraft with baselines comparable to Earth's diameter or greater (though there likely would be significant technical challenges regarding navigation and timing to be addressed).

The most familiar, and conceptually simplest, space-based concept is a monostatic radar instrument aboard either a dedicated craft or as part of a larger mission. Such instruments can penetrate atmospheres that are opaque at visible wavelengths and detect water or ice beneath rocky surfaces. Many such instruments have already flown successfully, including the *Apollo* lunar sounder (Porcello et al. 1974), the synthetic aperture radars aboard the Magellan (Pettengill et al. 1991) and *Cassini* (Elachi et al. 2004) spacecraft, the Mars Advanced Radar for Subsurface and Ionosphere Sounding (MARSIS) instrument aboard Mars Express (Picardi et al. 1999; Nielsen 2004), and the Shallow Radar (SHARAD) instrument (Biccari et al. 2002; Croci et al. 2007) aboard the Mars Reconnaissance Orbiter. Near-term radar instruments include the Radar for Europa Assessment and Sounding: Ocean to Near-Surface (REASON) instrument on Europa Clipper (Blankenship et al. 2024), the Venus Interferometric Synthetic Aperture Radar (VISAR) on NASA's Venus Emissivity, Radio Science, InSAR, Topography & Spectroscopy (VERITAS) mission¹ and the Synthetic Aperture Radar (VenSAR) on the ESA-led EnVision mission (Hensley et al. 2020). Compared with ground-based planetary radar, such systems can achieve higher resolution and signal-to-noise ratio, but the instruments must satisfy stringent power, thermal, and data volume requirements, and the missions have long lead times.

¹The Discovery-class VERITAS mission was selected shortly after the conclusion of this KISS study (Smrekar et al. 2022).

The KISS study group also discussed the possibility of a hybrid bistatic system, with high-power, high-gain illumination from Earth coupled with a receiver spacecraft in orbit around the target of interest, to receive and process radar echoes and relay the results to Earth. (This approach is sometimes termed “uplink bistatic radar.”) Because path losses in the radar equation would be reduced from $1/R^4$ to approximately $1/R^2$, this approach could be used to study distant objects, or to obtain high resolution or improve signal-to-noise ratio in a given integration time. It also avoids target visibility constraints from Earth rotation and would be unaffected by Earth-based radio-frequency interference. Recent applications of this approach include probing the surface of Vesta by the Dawn mission transmitting to DSN antennas (Palmer et al. 2017) and probing the atmosphere of Pluto by transmitting from a DSN antenna to the Radio Science Experiment (REX, Gladstone et al. 2016) on the New Horizons spacecraft.

A possible disruptive opportunity for uplink bistatic radar is the advent of relatively inexpensive small spacecraft operating beyond LEO. Multiple small spacecraft, each carrying an identical radar receiver, could be sent to different target bodies throughout the Solar System. While this architecture could reduce the power requirements on the individual small spacecraft, returning the required data volumes would remain a challenge. Should technologies identified under the KISS Nebula study (Vander Hook et al. 2020, 2021) be implemented, these could allow for increased on-board storage or processing or both, for small spacecraft at certain bodies (e.g., Venus, Mars). Longevity or reliability of spacecraft components and radiation tolerance requirements likely would remain challenging, though, as those requirements would significantly exceed those for spacecraft in LEO. The KISS study group also discussed briefly a concept in which multiple targets would be observed with a constellation of inexpensive small spacecraft, perhaps with a “mother” spacecraft to centralize communications and control.

3.5 Cross-Cutting Considerations

3.5.1 Spectrum Management

One of the scientific considerations is “wavelength (or frequency) diversity” (§2.5) in order to obtain better characterizations of targets. In addition to scientific considerations for a future ground-based planetary radar system, there are spectrum management considerations. There are many users of the radio spectrum, and the use of the radio spectrum is coordinated internationally through the International Telecommunications Union² (ITU), an agency that operates under the auspices of the United Nations. The ITU makes recommendations about which frequencies should be used for what purposes, with those recommendations taken into consideration by nations (“Member States”) for implementation.

Planetary radar transmissions are considered part of the more general Radiolocation Service, and there are a variety of frequency bands for which the Radiolocation Service is one of the recommended uses. For instance, the GSSR transmits with a central frequency of 8560 MHz with a bandwidth up to 50 MHz. There are two bands (8500 MHz–8550 MHz and 8550 MHz–8650 MHz), recommended both internationally and within the U.S., for which a primary service is Radiolocation.³ In general, for the range of frequencies discussed at the KISS workshop, there would be one or more appropriate frequencies to use for Radiolocation, thereby permitting a future planetary radar system.

3.5.2 Solid State Transmitters

For over a century, vacuum tube amplifiers have served as the standard source for high-power radio frequency (RF) signals used in communications and radar transmitter systems, including the current ground-based planetary radar systems (Table 3.1). Specifically, klystron tubes are typically used for applications from the ultra-high frequency (UHF) up to around 200 GHz. Within this frequency range and for relatively narrowband applications, klystrons

²<https://www.itu.int/>

³There are several countries for which additional services have allocations for all or part of this frequency range.

are unparalleled in their RF output power capability, gain, and efficiency. Klystron tubes can output, depending on frequency, anywhere from kilowatts to megawatts of continuous-wave RF output power, and 60 dB of gain is not uncommon. As a specific planetary radar example, the GSSR uses two klystrons, each producing approximately 250 kW of output power. Despite their tremendous power advantage over other technologies, their implementation presents challenges.

One such challenge is the often limited lifetime and reliability of these devices. Klystrons amplify a small input signal using a high-density electron beam. Beam formation requires the use of a high-potential electron gun, and this high-voltage requirement adds size and complexity to the transmitter and associated power supply. Additionally, typical klystron efficiency does not exceed 50%. When coupled with the large power densities within the electron beam, localized heating tends to limit lifetime and reliability for the high-power-class and higher-frequency klystrons.

Other challenges arise from the complex nature of the devices. Klystrons must be custom designed for a given frequency of operation, and typically require specialized tuning once they are assembled. Consequently, large scale and timely manufacturability can be difficult. There are only a handful of vendors worldwide with the capability and infrastructure to develop these devices. New designs can take months to years to refine, and costs for a new design can range from hundreds of thousands to a few million dollars. Klystron failures are typically catastrophic, requiring immediate replacement by a spare in order to prevent significant transmitter downtimes. If repair is possible, repair times typically take several months, and costs are usually a significant portion of the cost for a new klystron.

Though vacuum tube amplifiers are not likely to disappear anytime soon, recent advances in solid-state amplifier technology are providing a potential alternative to the use of vacuum tubes for high-power transmitter systems. While individual solid-state transistors are orders of magnitude lower in output power compared with tube amplifiers, techniques for combining many of these devices in parallel make it possible to achieve comparable output power and efficiencies. Solid-state transmitter systems are a technology that has been steadily maturing over the past two decades, with systems having been implemented in radar and communications systems across multiple industries, such as civilian and military aircraft, telecommunications, including wireless/cell phone technology (5G), and spacecraft. Notably, a 30 kW system operating at approximately 7 GHz has been implemented at the Misasa Deep Space Station of the Japan Aerospace Exploration Agency (JAXA, Nakahara et al. 2021), and, concurrently, there has been development at JPL of a solid-state transmitter module, targeted specifically at ground-based planetary radar applications (Figure 3.4).

Solid-state based transmitter systems provide specific advantages over tube-based systems. The lifetime and reliability of solid-state devices is a vast improvement over that of tubes. Additionally, the modular nature of solid-state power amplifiers (SSPAs) and large number of elements in parallel allow for the design of robust transmitters that exhibit graceful degradation as opposed to catastrophic failure. Both of these aspects together provide for a reduction of transmitter maintenance time and costs. Solid-state devices also are generally low-voltage devices that do not require high-voltage infrastructure and power supplies, which are considerably larger and require significant safety considerations. Solid-state transmitter technology comes with its own challenges, however. The technology is relatively new in comparison to tube amplifiers, and development efforts to improve efficiency, combining techniques, power output, scaling, higher frequency, and costs are ongoing.

The elemental and modular nature of SSPAs makes them well suited to developing radar techniques such as antenna and panel-style active phased array transmitting. The concurrent development of SSPA technology alongside transmit array technology is complementary, and it is foreseeable that solid-state transmitter systems will play a significant role in the next-generation planetary radar assets over the coming decades.

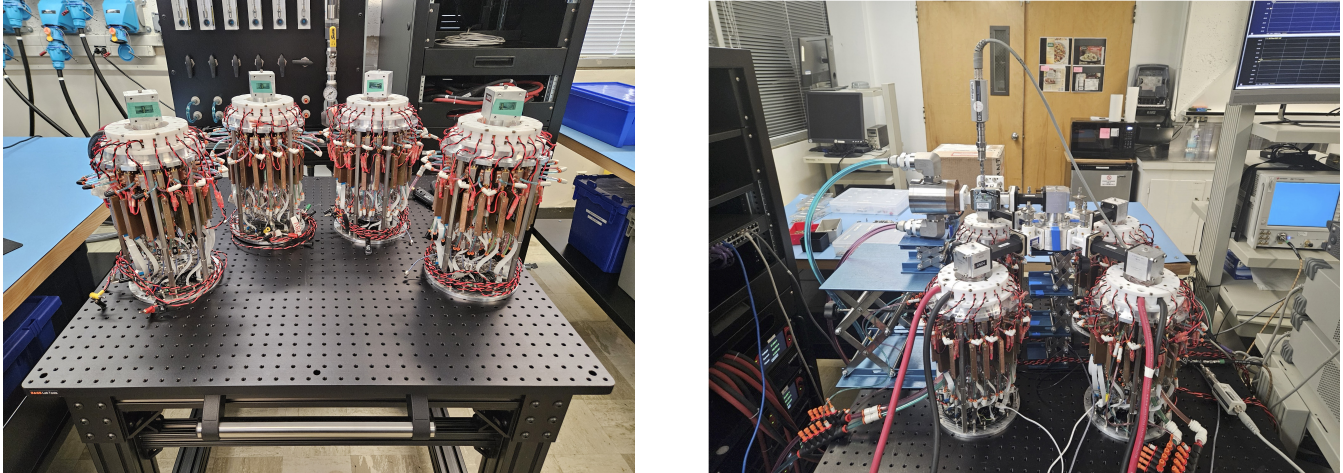


Figure 3.4: (left) Prototype planetary radar solid-state transmitter modules. Each module contains 16 commercially available amplifiers, each of which produces approximately 80 W of output power. A module (spatially) combines these 16 outputs to produce 1.1 kW of output power. (Each module is approximately 30 cm high.) (right) Combined together, individual solid-state modules can be the foundation of a future planetary radar transmitter. Four solid-state modules combined (radially) in a JPL laboratory have demonstrated over 4 kW of output power. This architecture is scalable, e.g., a 48 kW transmitter could be produced by a 16×4 kW system. (Credit: M. Taylor)

3.5.3 Automation and Rapid Turnaround

The growth of automation in the astronomy and space tracking communities lends many approaches for making planetary and asteroid radar observations more efficient. This is especially true for systems that are not dedicated to radar observations, such as the re-use of astronomical (GBT, Parkes) and space tracking facilities (DSN).

Rapid and Efficient Scheduling

Monostatic and bistatic radar facilities all operate within a schedule of usage. In the case of the DSN, this process involves negotiation and agreement between all missions (including the GSSR) over the weeks to months before the week during which an observation occurs. In the case of Arecibo, last-minute changes in the schedule were possible and urgent proposals for newly discovered asteroids were frequently submitted and quickly approved, requiring only internal communication between operations and observers. However, there was still the need to have an available telescope operator and scientist for the observation to be possible. Reducing this interval to hours would be valuable for surprise or urgent targets such as recently discovered asteroids. Automated scheduling also would allow responding to alert streams that are and will be generated by various sky surveys (e.g., Carrasco-Davis et al. 2021).

Rapid scheduling for bistatic systems can be more difficult than for monostatic systems, as it requires coordination and scheduling of both transmit and receive facilities. Rapid scheduling has been achieved at bistatic radars such as the DSN and the ATNF (Australia Telescope National Facility), but at the expense of “bumping” observers off an instrument. While this technique is feasible at radio astronomical telescopes—many radio astronomical observations are not time-critical, so they can be deferred for a rapid response observation—this approach is less feasible at space tracking facilities (the DSN) due to the significant advance planning that can be required for spacecraft telecommunications. One approach would be to insert dynamically-scheduled “blocks” into antenna schedules, allowing responses to recently-discovered asteroids. This approach does require some optimization between the demands of various missions, as well as to ensure that there are not so many blocks that there are not a sufficient number of radar targets. Hackett et al. (2021) describes an approach to “on-demand” DSN scheduling, which may have significant applicability to rapid radar scheduling.

Automation of Antenna Setup

The manual process of antenna and transmitter setup is still a “feature” of planetary radars. By contrast, considerable automation is present in spacecraft tracking, for at least low-Earth orbit spacecraft. Automation offers the potential of an increase, possibly a dramatic increase, in the number of targets without the cost of an entirely new facility.

Examples of processes that could be automated include the following:

- Asteroid astrometry data could be converted to antenna setup and track commands; this capability exists partially, but further development is feasible.
- A radar track can consist of over 200 individual commands, many of which could be scripted or combined, particularly to ensure safe and repeatable observations.
- Replacing analog equipment that requires manual configuration or cabling with digital equipment that can be controlled automatically could both make changing radar configurations more efficient and mitigate problems with equipment such as bad cables or any human errors.

Initial Signal Detection

The detection of a radar echo is achieved by signal correlation, often with a low S/N ratio, and dependent upon coordinated pointing of the transmitter and receiver. In both monostatic and bistatic systems, coordinated pointing requires precise geographic centers of the transmit and receive elements. The above is made more efficient when there is real-time communication between the observer and operator, and especially for bistatic radar between transmitter and receiver sites. Adding further automation of target search and “handshaking” between sites would minimize the risk of missing the target and maximize effective use of observing time.

Data Analysis and Advanced Techniques

Automation of data analysis for echo signal detection in real time, or near-real time, is a desired means that has been achieved to various degrees. Manual detection is still the norm at some sites (e.g., DSN-ATNF bistatic system). Automating the initial analysis of radar returns promises improved peak detection and the potential for feature detection, such as whether an asteroid target is a binary. At the GSSR, and formerly at Arecibo, the process of confirming a signal detection, deciding if a correction for the Doppler shift or delay or both is needed, choosing and applying the correction, and generating and updating the ephemeris are all done manually. Radar observations would benefit from automated astrometry, making it possible to quickly switch to the next observation setup or target.

Generation of higher-order data products such as Doppler broadening vs. rotational period, ratios of spin moments of inertia, range resolution, and even target image generation and analysis may be feasible with advances in software. In some cases, full automation may not be required or even desirable, but even supervised automation could result in substantial efficiencies. For instance, initial investigations conducted under the auspices of the Frontier Development Lab (FDL) suggested that asteroid shape models could be developed much more rapidly by employing generative adversarial networks (GANs).⁴

Speckle Tracking

For future speckle tracking observations of asteroids or close-passing comets with unknown spin states, the primary requirement is a set of receive antennas with a wide range of baseline lengths and angles (§3.1.1). For current observations, the VLBA provides this capability; there have been discussions about what antennas could be used in the southern hemisphere to receive transmissions from an antenna at the DSN Canberra Complex in order to provide a similar capability, but there have been no such observations conducted to date. In the future, the ngVLA would provide this capability in the northern hemisphere.

⁴<https://fdl.ai/fdl-2017>

A higher-power radar facility would permit unprecedented spin state studies of the Galilean satellites and potentially even the largest few Main Belt objects. Such observations would provide moment-of-inertia measurements and constrain their internal structures. In the case of Europa, speckle observations could measure libration of the ice shell relative to the rest of the moon and constrain its mass and thickness. Speckle tracking observations of Mars are, in principle, possible but seem unlikely to provide information about Mars' spin state and interior beyond that provided by current and expected future Mars spacecraft.

3.5.4 Longitudinally-Spaced Transmitters and Global Coordination

The long-term values from regional and global planetary radar observation coordination include improved characterization potential, all-sky coverage, and resiliency. Sites distributed in longitude would ensure full (or nearly full) asteroid rotation coverage while they are close enough to detect. Increased coverage of their rotational phases improves shape modeling and would enable studies of variations in surface properties as a function of location on their surfaces. For those asteroids with satellites, sites distributed in longitude would increase the fractions of orbital periods that could be monitored, thereby improving estimates of the primary asteroids' masses and (bulk) densities. Capabilities in both the northern and southern hemispheres would improve the astrometry and orbit determinations for asteroids that approach from one hemisphere and recede from the other. At the most extreme case, Giorgini et al. (2009) shows that up to 5% of a population of asteroids on impacting trajectories would be observable only from the southern hemisphere in the decades before impact and could not be tracked with sufficient fidelity with only a northern hemisphere system. In the case of observations of Venus, determinations of its spin state and moment of inertia require distributed (receiving) sites (Margot et al. 2021).

From a technical or engineering perspective, having coordinated transmissions or receptions at multiple sites is often a technique used to verify the performance of a system, particularly a new or upgraded system. This technique has been used to confirm performance in the context of planetary radar capabilities (e.g., Benson et al. 2017; Di Martino et al. 2004).

All antennas must (or should) undergo regular maintenance, during which they cannot be used for transmission or reception. Having multiple sites improves resiliency by ensuring that, even if one site is unable to operate, for whatever reason, another site still can conduct observations. An example of the value of multiple sites occurred during 2021 when the GSSR was undergoing maintenance, but the DSN-ATNF bistatic system was able to conduct observations of a number of asteroids, including (332446) 2008 AF₄ and (231937) 2001 FO₃₂. A future such example is that the GSSR will be undergoing significant maintenance and modernization of its systems from approximately mid-2026 to late 2028, during which time it largely will be unavailable.

3.5.5 Surveys

Standard planetary radar observations are conducted only if the target orbit knowledge is precise enough to predict the sky location much better than the antenna beam diameter. The GSSR (70 m antenna transmitting at 3.5 cm wavelength, Table 3.1), produces a beam diameter of approximately 1.7' (0.03° or 0.5 milliradians). This requirement poses no constraints for planetary observations, for which orbits are known to much better precision. However, it can limit asteroid observations, particularly newly discovered asteroids with poorly known orbits.

Radars commonly search for objects in other contexts. Perhaps the most famous such radar is the Space Fence (originally the Naval Space Surveillance system or NAVSPASUR), though its objects of interest have been and are *much* closer than planetary radar scenarios require. Nonetheless, potential advancement would involve developing techniques enabling near-Earth asteroid searches over modest sky areas, even without an all-sky "Asteroid Fence."⁵

⁵cf. the SPACEGUARD Project described in *Rendezvous with Rama*

An approach that may apply in certain scenarios, such as searching for minimoons (§2.2.1; Jedicke et al. 2018), would occur if there are only limited orbital phase regions in space that are relevant. Brozović et al. (2017) demonstrated Chandrayaan-1 spacecraft recovery in lunar orbit because only its orbital phase about the Moon was unknown.



4. Ground-Based Planetary Radar Futures

Ground-based planetary radars played an integral role in the laying the foundations of our understanding of the Solar System during the last half of the 20th Century. Planetary radar observations helped enable interplanetary missions, obtained the first surface composition characterizations across various Solar System bodies, and made fundamental planetary defense contributions. This contribution record continued through the first quarter of the 21st Century, though the Arecibo Observatory collapse took a significant toll. What could or should the remainder of the first half of the 21st Century hold for ground-based planetary radars?

Chapter 2 illustrates how the range of scientific investigations addressable by next-generation ground-based planetary radar touches upon numerous fundamental Planetary Science and planetary defense questions. At Venus (“Earth’s evil twin”), a next-generation ground-based planetary radar would provide long-term surface geology measurements and baseline measurements to contextualize data from the spacecraft suite planned to explore that planet over the next decade or more. A next-generation ground-based planetary radar would contribute to improved near-Earth asteroid population characterization by increasing the quantity of trackable near-Earth asteroids and improving the data quality (e.g., higher signal-to-noise ratio and higher resolution surface imaging). These systems would also provide precise orbit determinations for spacecraft mission planning and planetary defense hazard assessments. For the outer Solar System, a next-generation ground-based planetary radar could provide measurements of icy moons (“ocean worlds”) over unparalleled durations, enabling surface characterizations of moons that might be visited only briefly by spacecraft or tracking seasonal changes.

Chapter 3 shows that much of the technology for a next-generation ground-based planetary radar is maturing. Solid-state transmitters have been prototyped and, in one case, deployed for spacecraft telecommunications. Such solid-state transmitters leverage considerable commercial investments in solid-state technology and offer much more reliable performance than the traditional vacuum-tube klystrons. Antenna arrays, already a well-proven architecture for both radar and natural radio signal reception, have been demonstrated for transmission. Automation and new algorithms show considerable promise when scheduling observations and processing planetary radar data, even within existing systems.

The second KISS workshop concluded in 2021 May. Several notable developments related to the possible development of a next-generation ground-based planetary radar have since emerged. The ngRadar project for a new planetary radar system uses existing telescope infrastructure, specifically the Green Bank Telescope (GBT, §3.2), and is proceeding beyond the concept design phase. The objective involves greatly increasing output power from the initial 0.7 kW proof-of-concept system to approximately 500 kW transmit power, with potential Very Large Array (VLA) and future next-generation Very Large Array (ngVLA) use as receivers to further improve ngRadar system sensitivity.

The National Academies released *Origins, Worlds, and Life: A Decadal Strategy for Planetary Science and Astrobiology 2023–2032*, charting an ambitious planetary exploration course over the next decade and beyond. Among its recommendations was the following (emphasis original):

Recommendation: NASA and NSF should review the current radar infrastructure to determine how best to meet the community’s needs, including expanded capabilities at existing facilities, to replace those lost with Arecibo.

This recommendation led to the “Cross-Disciplinary Deep Space Radar Needs Study” (Marshall et al. 2023). That study developed use cases involving both Planetary Science (including planetary defense) and space situational awareness (SSA), engaging with subject matter experts, including several participants in this KISS study, to review current capabilities, the state of practice, and future possibilities. The study found that current ground-based planetary radar capabilities can respond to a significant use case subset and that technically feasible near-term and longer-term options exist for addressing all identified use cases. All technically feasible future options involve technologies discussed within this KISS workshop.

Sánchez Net et al. (2022) conducted an initial concept study for a ground-based planetary radar array, inspired partly by this KISS study and somewhat concurrent with the “Cross-Disciplinary Deep Space Radar Needs Study” (Marshall et al. 2023), focused on asteroid or other small body observations. This concept study conducted a trade study of potential different designs—considering different antenna diameters, transmitter powers, and required antenna numbers in the array—aiming to find an optimum design in a Pareto sense while considering life-cycle costs.

Both the “Cross-Disciplinary Deep Space Radar Needs Study” (Marshall et al. 2023) and the Sánchez Net et al. (2022) concept study concluded that an antenna array with diameters ranging from 15 m to 25 m and equipped with transmitters with output powers in the range of 50 kW to 80 kW could respond to all use cases identified. Previously, Statman et al. (2004) had considered life-cycle costs for an antenna array intended for spacecraft telecommunications and reached similar conclusions. The parameter ranges differ slightly based on the two studies’ assumptions, but they remain notably consistent with each other and with the KISS study discussions.

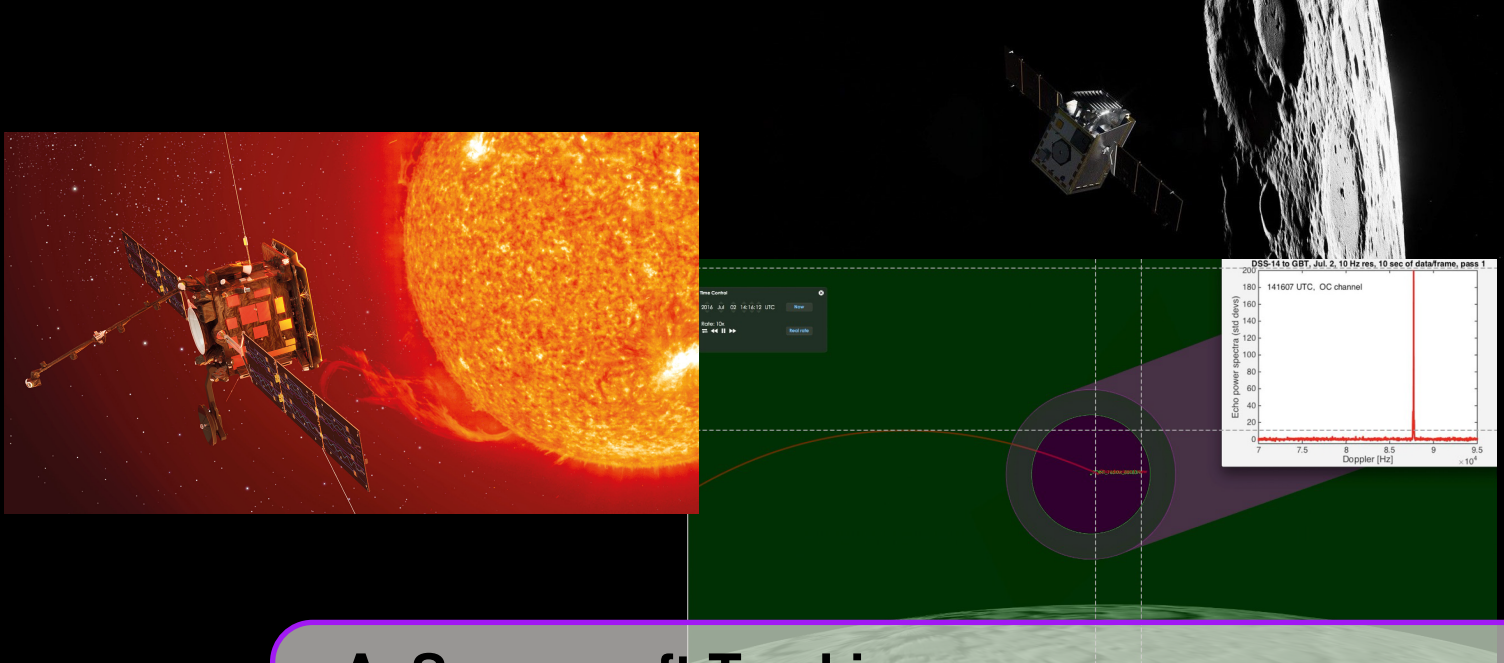
On the same time scale as this KISS study and the *Origins, Worlds, and Life* (2022) report, the Deep Space Advanced Radar Capability (DARC) test array was demonstrated,¹ though its primary focus was on use cases other than Planetary Science, and China announced plans for an asteroid radar array. Due to the nature of both projects, less information is available in open literature, but they both illustrate the feasibility of next-generation, ground-based planetary radar arrays.

The most significant challenge for a next-generation, ground-based planetary radar is neither scientific nor technical, but programmatic. Multiple facets exist for the programmatic concerns associated with next-generation, ground-based planetary radar. The “Cross-Disciplinary Deep Space Radar Needs Study” (Marshall et al. 2023) noted, “NASA does not develop ground-based facilities of its own [and] NSF’s scope does not include development of planetary defense or cislunar SSA facilities.” Both the “Cross-Disciplinary Deep Space Radar Needs Study” (Marshall et al. 2023) and the Sánchez Net et al. (2022) concept study developed initial cost estimates for next-generation, ground-based planetary radar arrays, though they approached the cost estimates differently. The “Cross-Disciplinary

¹<https://www.jhuapl.edu/destinations/missions/darc-demonstration>

Deep Space Radar Needs Study” (Marshall et al. 2023) focused primarily on construction costs, while the Sánchez Net et al. (2022) concept study considered life-cycle costs but did not include site development costs. Nonetheless, their conclusions were similar—a next-generation, ground-based planetary radar array would cost at least hundreds of millions of dollars, and the most capable planetary radar array designs have estimated costs exceeding \$1 billion (\$1,000,000,000).

A facility of this scale is completely feasible, as numerous other ground-based telescopes are comparable or even larger in scale. Such facilities have multiple partners for both construction and operations costs, which would likely be required for a next-generation, ground-based planetary radar. A desirable next step toward realizing such a facility would be a more detailed concept study report, developing more robust technical implementation and cost estimates than those developed in this report, the “Cross-Disciplinary Deep Space Radar Needs Study” (Marshall et al. 2023), or the Sánchez Net et al. (2022) concept study.



A. Spacecraft Tracking

The same radar capabilities required to observe Solar System bodies also enable spacecraft tracking at the Moon and beyond, though this was not a workshop focus. These observation capabilities have proven crucial for characterizing spacecraft that have developed onboard problems and have contributed to saving at least one mission. Lazio et al. (2022) discusses in more detail the potential capabilities of ground-based planetary radars in this context, with aspecific focus on spacecraft around or near the Moon. Here, we illustrate with notable examples.

Solar and Helio physics Observatory (SOHO) This joint European Space Agency-NASA mission launched in 1995 to an orbit about the Sun-Earth Lagrange 1 point for continuous solar viewing. Radio contact with the spacecraft was lost in 1998 June. A series of bistatic radar observations with the Arecibo Observatory transmitting and the Goldstone Solar System Radar receiving confirmed that the spacecraft remained in its nominal orbit and determined its attitude.¹

Chandrayaan-1 This Indian Space Research Organization lunar-orbiting spacecraft operated from 2008 to late 2009, when radio communications with the spacecraft were lost. It was assumed that the spacecraft had crashed into the Moon. Subsequent investigation revealed that the spacecraft still might be in orbit. A bistatic radar observation with the Goldstone Solar System Radar transmitting and the Green Bank Telescope receiving detected the spacecraft and determined its orbital phase (Brozović et al. 2017).

Lunar Trailblazer The Lunar Trailblazer mission was launched during the final stages of this report. One day later, radio communications with the spacecraft were lost shortly after placement onto its lunar trajectory. Over the course of approximately a week, radar observations were conducted using the Goldstone Solar System Radar, the Deep Space Network's research and development antenna Deep Space Station-13, and the Green Bank Telescope (Figure A.1). These radar observations provided the first spacecraft trajectory determinations, confirming that it was en route to the Moon and providing crucial orbital information for its Moon flyby. The received power levels from the spacecraft also varied over the course of a track. This information, combined with ground-based visible-wavelength telescope observations, helped to assess the spacecraft's attitude as part of the mission recovery efforts. Results of these observations have been submitted for publication.

¹"SOHO spacecraft located with ground-based radar,"

<https://sohowww.nascom.nasa.gov/newsroom/oldesapr/press27.html>

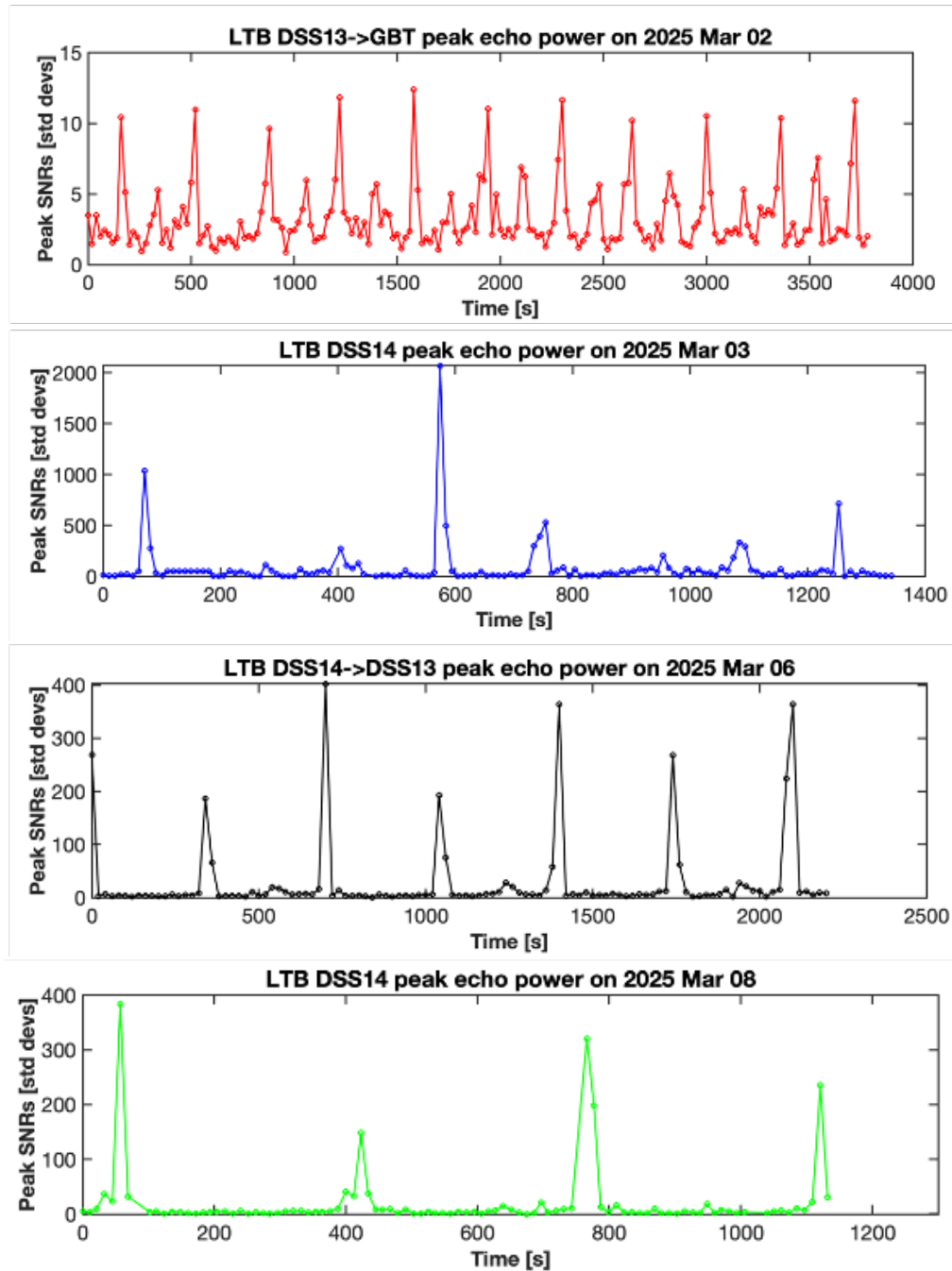
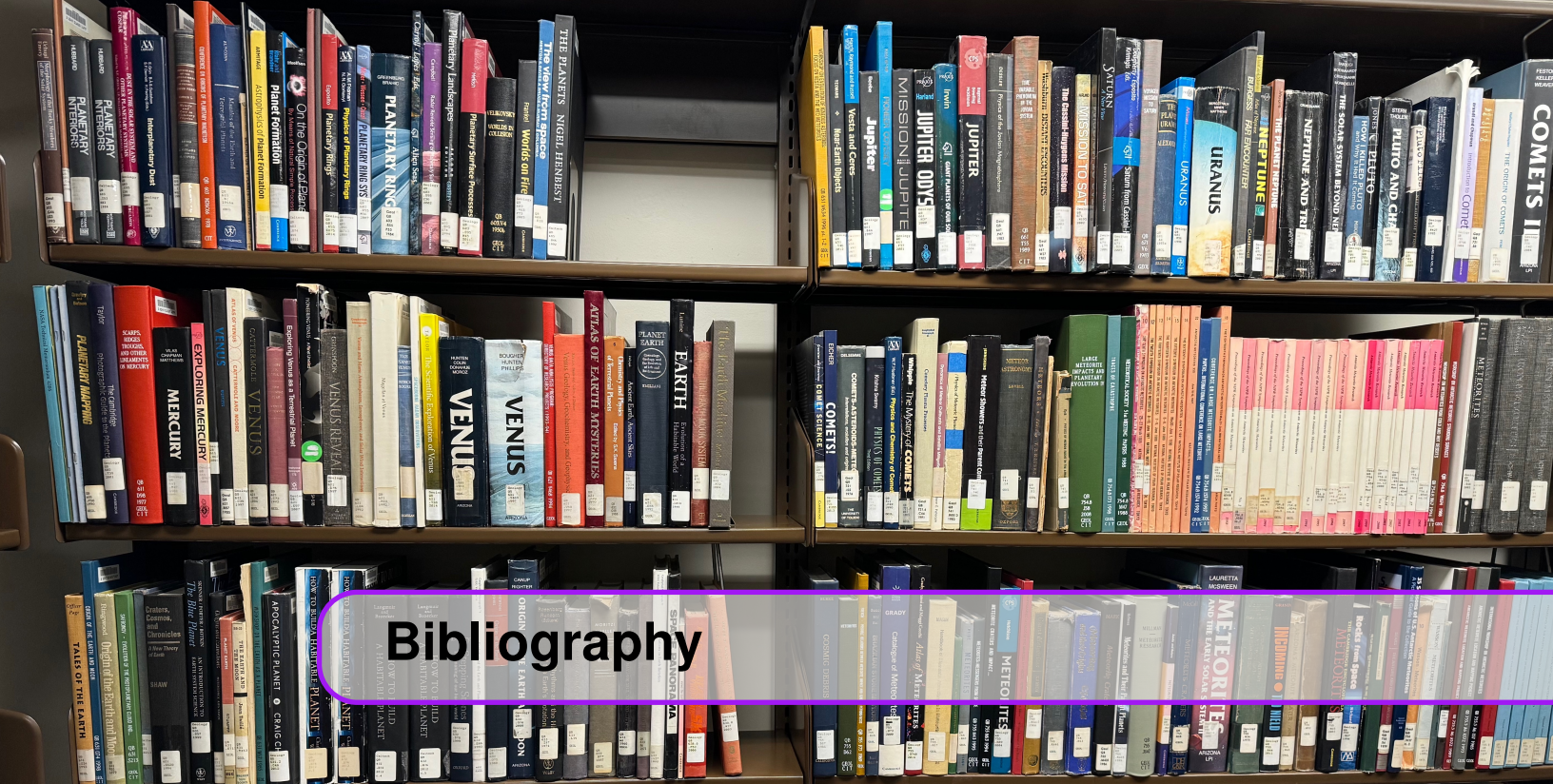


Figure A.1: Bistatic radar observations used to track the Lunar Trailblazer spacecraft. From top to bottom, the plots show the received power as a function of time for radar observations on 2025 March 2 (en route to the Moon, Deep Space Station-13 [DSS-13] transmitting-Green Bank Telescope receiving [GBT]), March 3 (en route to the Moon, DSS-14/Goldstone Solar System Radar [GSSR]), March 6 (after Moon fly-by, DSS-14/GSSR transmitting-DSS-13 receiving), and March 8 (after Moon fly-by, DSS-14/GSSR). The variations in power levels are real and likely represent a change in effective radar cross section due to the spacecraft's rotation. Note that the durations of the radar tracks vary from day to day.



Bibliography

- A'Hearn, M. F., Belton, M. J. S., Delamere, W. A., et al. 2011, *Science*, 332, 1396
- Asphaug, E., Ryan, E. V., & Zuber, M. T. 2002, in *Asteroids III*, ed. W. F. Bottke Jr., A. Cellino, P. Paolicchi, & R. P. Binzel (Tucson, AZ: University of Arizona Press), 463–484
- Bagenal, F., Dowling, T. E., & McKinnon, W. B. 2004, *Jupiter : the planet, satellites and magnetosphere* (Cambridge, UK: Cambridge University Press)
- Baker, D. M. H., Haltigin, T., Viotti, M. A., et al. 2024, in *LPI Contributions*, Vol. 3040, 55th Lunar and Planetary Science Conference, 2506
- Barnes, J. W., Turtle, E. P., Trainer, M. G., et al. 2021, *Plan. Sci. J.*, 2, 130
- Bauer, J. M., Grav, T., Blauvelt, E., et al. 2013, *ApJ*, 773, 22
- Benner, L. A. M., Busch, M. W., Giorgini, J. D., Taylor, P. A., & Margot, J. L. 2015, in *Asteroids IV* (Tucson, AZ: University of Arizona Press), 165–182
- Benson, C., Reynolds, J., Stacy, N. J. S., et al. 2017, *Radio Science*, 52, 1344
- Biccari, D., Picardi, G., & Seu, R. 2002, in *IEEE International Geoscience and Remote Sensing Symposium*, Vol. 4, 2159–2161
- Black, G. J., Campbell, D. B., & Carter, L. M. 2011, *Icarus*, 212, 300
- Black, G. J., Campbell, D. B., & Harmon, J. K. 2010, *Icarus*, 209, 224
- Blankenship, D. D., Moussessian, A., Chapin, E., et al. 2024, *Space Sci. Rev.*, 220, 51
- Bolin, B. T., Delbo, M., Morbidelli, A., & Walsh, K. J. 2017, *Icarus*, 282, 290

- Bolin, B. T., Morbidelli, A., & Walsh, K. J. 2018, *A&A*, 611, A82
- Bonsall, A., Watts, G., Lazio, J., et al. 2019, in *Bulletin of the American Astronomical Society*, Vol. 51, 208
- Brearley, A. J. 2006, in *Meteorites and the Early Solar System II*, ed. D. S. Lauretta & H. Y. McSween (Tucson, AZ: University of Arizona Press), 584
- Brown, M. E., & Fraser, W. C. 2023, *Plan. Sci. J.*, 4, 130
- Brown, S., Zhang, Z., Bolton, S., et al. 2023, *Journal of Geophysical Research (Planets)*, 128, e2022JE007609
- Brozović, M., Butler, B. J., Margot, J., Naidu, S. P., & Lazio, T. J. W. 2018a, in *Astronomical Society of the Pacific Conference Series*, Vol. 517, *Science with a Next Generation Very Large Array*, ed. E. Murphy, 113
- Brozović, M., Park, R. S., McMichael, J. G., et al. 2017, in *26th International Symposium on Space Flight Dynamics*, iSTS-2017-d-107/ISSFD-2017-107
- Brozović, M., Benner, L. A. M., McMichael, J. G., et al. 2018b, *Icarus*, 300, 115
- Burns, J. A., & Matthews, M. S. 1986, *Satellites* (Tucson, AZ: Univ. of Arizona Press)
- Busch, M. W., Kulkarni, S. R., Briskin, W., et al. 2010, *Icarus*, 209, 535
- Busch, M. W., Ostro, S. J., Benner, L. A. M., et al. 2007, *Icarus*, 186, 581
- Butler, B. J., Muhleman, D. O., & Slade, M. A. 1993, *Journal of Geophysical Research*, 98, 15003
- Camarca, M., de Kleer, K., Butler, B., et al. 2023, *Plan. Sci. J.*, 4, 142
- Campbell, B. A., & Campbell, D. B. 2022, *Plan. Sci. J.*, 3, 55
- Campbell, B. A., Campbell, D. B., Chandler, J. F., et al. 2003a, *Nature*, 426, 137
- Campbell, D. B., Black, G. J., Carter, L. M., & Ostro, S. J. 2003b, *Science*, 302, 431
- Campbell, D. B., Chandler, J. F., Pettengill, G. H., & Shapiro, I. I. 1977, *Science*, 196, 650
- Carrasco-Davis, R., Reyes, E., Valenzuela, C., et al. 2021, *AJ*, 162, 231
- Carruba, V., Aljbaae, S., & Lucchini, A. 2019, *MNRAS*, 488, 1377
- Chabot, N. L., Ernst, C. M., Denevi, B. W., et al. 2012, *Geophysical Research Letters*, 39, L09204
- Chodas, P. 2019, in *EPSC-DPS Joint Meeting 2019*, Vol. 2019, EPSC–DPS2019–1919
- Croci, R., Fois, F., Calabrese, D., et al. 2007, in *2007 IEEE International Geoscience and Remote Sensing Symposium*, 1611–1615
- D’Addario, L., Proctor, R., Trinh, J., Sigman, E., & Yamamoto, C. 2009, *Interplanetary Network Progress Report*, 42-176, 1
- D’Addario, L. R. 2008, *Interplanetary Network Progress Report*, 42-175, 1
- de Kleer, K., Butler, B., de Pater, I., et al. 2021, *Plan. Sci. J.*, 2, 5
- de Kleer, K., & de Pater, I. 2017, *Icarus*, 289, 181

-
- de Leon, J., Pinilla-Alonso, N., Sarid, G., De Prá, M., & Lorenzi, V. 2019, in EPSC-DPS Joint Meeting 2019, Vol. 2019, EPSC–DPS2019–1147
- de Pater, I., de Kleer, K., Davies, A. G., & Ádámkovics, M. 2017, *Icarus*, 297, 265
- de Pater, I., Luszcz-Cook, S., Rojo, P., et al. 2020, *Plan. Sci. J.*, 1, 60
- De Prá, M. N., Licandro, J., Pinilla-Alonso, N., et al. 2020a, *Icarus*, 338, 113473
- De Prá, M. N., Pinilla-Alonso, N., Carvano, J. M., et al. 2018, *Icarus*, 311, 35
- De Prá, M. N., Pinilla-Alonso, N., Carvano, J., et al. 2020b, *A&A*, 643, A102
- Delbo', M., Walsh, K., Bolin, B., Avdellidou, C., & Morbidelli, A. 2017, *Science*, 357, 1026
- Deutsch, A. N., Chabot, N. L., Mazarico, E., et al. 2016, *Icarus*, 280, 158
- Di Martino, M., Montebugnoli, S., Cevolani, G., et al. 2004, *Plan. Space Sci.*, 52, 325
- Elachi, C., Allison, M. D., Borgarelli, L., et al. 2004, *Space Sci. Rev.*, 115, 71
- Eubanks, T. M., Hein, A. M., Lingam, M., et al. 2021, arXiv e-prints, arXiv:2103.03289
- Genda, H., Usui, T., Chabot, N. L., Ramirez, R., & Ohtsuki, K. 2024, *Earth, Planets and Space*, 76, 8
- Giorgini, J. D., Benner, L. A. M., Brozović, M., et al. 2009, Radar Astrometry of Small Bodies: Detection, Characterization, Trajectory Prediction, and Hazard Assessment, Tech. rep., Jet Propulsion Laboratory, National Aeronautics and Space Administration, White Paper, submitted to the Planetary Sciences Decadal Survey (2013–2022). <https://trs.jpl.nasa.gov/handle/2014/45703>
- Gladstone, G. R., Stern, S. A., Ennico, K., et al. 2016, *Science*, 351, aad8866
- Grav, T., Mainzer, A. K., Bauer, J. M., Masiero, J. R., & Nugent, C. R. 2012a, *ApJ*, 759, 49
- Grav, T., Mainzer, A. K., Bauer, J., et al. 2012b, *ApJ*, 744, 197
- Hackett, T. M., Johnston, M. D., Wyatt, E. J., & Bilén, S. G. 2021, in 16th International Conference on Space Operations (Cape Town, South Africa: SpaceOps)
- Harcke, L. J. 2005, PhD thesis, Stanford University, California
- Harmon, J. K. 2002, *IEEE Trans. Geosci. Remote Sensing*, 40, 1904
- Harmon, J. K., Campbell, D. B., Ostro, S. J., & Nolan, M. C. 1999, *Plan. Space Sci.*, 47, 1409
- Harmon, J. K., Nolan, M. C., Howell, E. S., Giorgini, J. D., & Taylor, P. A. 2011, *ApJ*, 734, L2
- Harmon, J. K., Nolan, M. C., Husmann, D. I., & Campbell, B. A. 2012, *Icarus*, 220, 990
- Harmon, J. K., Nolan, M. C., Ostro, S. J., & Campbell, D. B. 2004, in *Comets II*, ed. M. C. Festou, H. U. Keller, & H. A. Weaver (Tucson, AZ: University of Arizona Press), 265
- Harmon, J. K., & Slade, M. A. 1992, *Science*, 258, 640
- Harmon, J. K., Slade, M. A., Butler, B. J., et al. 2007, *Icarus*, 187, 374
- Harmon, J. K., Slade, M. A., Vélez, R. A., et al. 1994, *Nature*, 369, 213

- Haynes, M. S., Bernhardt, P. A., Benner, L. A. M., et al. 2023, in 2023 XXXV General Assembly and Scientific Symposium of the International Union of Radio Science (URSI GASS), 1–4
- Hensley, S., Campbell, B., Perkovic-Martin, D., et al. 2020, in 2020 IEEE Radar Conference (RadarConf20), 1–6
- Hirayama, K. 1918, *AJ*, 31, 185
- Hofgartner, J. D., Hayes, A. G., Campbell, D. B., et al. 2020, *Nature Communications*, 11, 2829
- Holin, I. V. 2010, *Icarus*, 207, 545
- Jedicke, R., Bolin, B. T., Bottke, W. F., et al. 2018, *Frontiers in Astronomy and Space Sciences*, 5, 13
- Jewitt, D. 2012, *AJ*, 143, 66
- Jewitt, D., Hsieh, H., & Agarwal, J. 2015, in *Asteroids IV*, ed. P. Michel, F. E. DeMeo, & W. F. Bottke, 221–241
- Jonas, J., & MeerKAT Team. 2016, in *MeerKAT Science: On the Pathway to the SKA*, 1
- Kamoun, P., Campbell, D., Pettengill, G., & Shapiro, I. 1998, *Plan. Space Sci.*, 47, 23
- Kamoun, P., Lamy, P. L., Toth, I., & Herique, A. 2014, *A&A*, 568, A21
- Kholin, I. V. 1992, *Radiophysics and Quantum Electronics*, 35, 284
- Knežević, Z. 2016, in *Asteroids: New Observations, New Models*, ed. S. R. Chesley, A. Morbidelli, R. Jedicke, & D. Farnocchia, Vol. 318, 16–27
- Kofman, W., Herique, A., Barbin, Y., et al. 2015, *Science*, 349, 2.639
- Kooi, J., Soriano, M., Bowen, J., et al. 2023, *IEEE Journal of Microwaves*, 3, 570
- Lawrence, D. J., Feldman, W. C., Goldsten, J. O., et al. 2013, *Science*, 339, 292
- Lazio, T. J. W., Antsos, D., Beasley, A., et al. 2022, in *Advanced Maui Optical and Space Surveillance Technologies Conference*, Maui Economic Development Board (Maui, Hawai'i: Maui Economic Development Board)
- Levasseur-Regourd, A. C., Hadamcik, E., & Lasue, J. 2006, *Advances in Space Research*, 37, 161
- Lopes, R., de Kleer, K., & Keane, J. 2023, *Astrophysics and Space Science Library*, Vol. 468, *Io: A New View of Jupiter's Moon* (New York: Springer), doi:10.1007/978-3-031-25670-7
- Lora, J. M., Lunine, J. I., & Russell, J. L. 2015, *Icarus*, 250, 516
- Lunine, J. I. 2006, *Origin of Water Ice in the Solar System*, ed. D. S. Lauretta & H. Y. McSween (Tucson, AZ: Univ. of Arizona Press), 309
- Margot, J.-L., Campbell, D. B., Giorgini, J. D., et al. 2021, *Nature Astronomy*, 5, 676
- Margot, J. L., Peale, S. J., Jurgens, R. F., Slade, M. A., & Holin, I. V. 2007, *Science*, 316, 710
- Marshall, M. F., Schnee, S. L., Cruz-Klueber, V., et al. 2023, *Cross-Disciplinary Deep Space Radar Needs Study*, Tech. Rep. ATR-2023-01267, Aerospace Corp., prepared for: Planetary Defense Coordination Office, Planetary Science Division, Science Mission Directorate (SMD); Contract No. 80GSFC19D0011
- Masiero, J. R., DeMeo, F. E., Kasuga, T., & Parker, A. H. 2015, *Asteroid Family Physical Properties* (Tucson, AZ: University of Arizona Press), 323–340

- Milani, A., Cellino, A., Knežević, Z., et al. 2014, *Icarus*, 239, 46
- Muhleman, D. O., Butler, B. J., Grossman, A. W., & Slade, M. A. 1991, *Science*, 253, 1508
- Muhleman, D. O., Grossman, A. W., Butler, B. J., & Slade, M. A. 1990, *Science*, 248, 975
- Müller, T. G., Micheli, M., Santana-Ros, T., et al. 2023, *A&A*, 670, A53
- Müller, T. G., Lellouch, E., Böhnhardt, H., et al. 2009, *Earth Moon and Planets*, 105, 209
- Naidu, S. P., Benner, L. A. M., Margot, J.-L., Busch, M. W., & Taylor, P. A. 2016, *AJ*, 152, 99
- Naidu, S. P., Benner, L. A. M., Brozovic, M., et al. 2020, *Icarus*, 348, 113777
- Naidu, S. P., Chesley, S. R., Moskovitz, N., et al. 2024, *Plan. Sci. J.*, 5, 74
- Nakahara, T., Yamada, Y., Otake, T., et al. 2021, *NEC Technical Journal*, 16, 158, special Issue on Social Infrastructure that Guarantees Safety, Security, Fairness, and Efficiency
- Nan, R.-d., Zhang, H.-y., Zhang, Y., et al. 2017, *Chinese Astron. Astrophys.*, 41, 293
- National Academies of Sciences, Engineering, and Medicine. 2022, *Origins, Worlds, and Life: A Decadal Strategy for Planetary Science and Astrobiology 2023–2032* (The National Academies Press: Washington, DC), doi: 10.17226/26522
- National Research Council. 2010, *Defending Planet Earth: Near-Earth-Object Surveys and Hazard Mitigation Strategies* (The National Academies Press: Washington, DC), doi: 10.17226/12842
- Nesvorný, D., Brož, M., & Carruba, V. 2015, *Identification and Dynamical Properties of Asteroid Families* (Tucson, AZ: University of Arizona Press), 297–321
- Nesvorný, D., Jedicke, R., Whiteley, R. J., & Ivezić, Ž. 2005, *Icarus*, 173, 132
- Nesvorný, D., Roig, F., Vokrouhlický, D., & Broz, M. 2024, *ApJS*, in press
- Nielsen, E. 2004, *Space Sci. Rev.*, 111, 245
- Ostro, S. J. 2007, *Encyclopedia of the Solar System*, 2nd edition edn. (Elsevier, Inc.), 735–764
- Ostro, S. J., Jurgens, R. F., Yeomans, D. K., Standish, E. M., & Greiner, W. 1989, *Science*, 243, 1584
- Ostro, S. J., & Pettengill, G. H. 1978, *Icarus*, 34, 268
- Ostro, S. J., & Shoemaker, E. M. 1990, *Icarus*, 85, 335
- Palmer, E. M., Heggy, E., & Kofman, W. 2017, *Nature Communications*, 8, 409
- Pappalardo, R. T., McKinnon, W. B., & Khurana, K. K. 2009, *Europa* (Tucson, AZ: University of Arizona Press)
- Pettengill, G. H., & Dyce, R. B. 1965, *Nature*, 206, 1240
- Pettengill, G. H., Ford, P. G., Johnson, W. T. K., Raney, R. K., & Soderblom, L. A. 1991, *Science*, 252, 260
- Picardi, G., Sorge, S., Seu, R., et al. 1999, in *IEEE 1999 International Geoscience and Remote Sensing Symposium. IGARSS'99* (Cat. No.99CH36293), Vol. 5, 2674–2677

- Pinilla-Alonso, N., de León, J., Morate, D., et al. 2017, in AAS/Division for Planetary Sciences Meeting Abstracts, Vol. 49, AAS/Division for Planetary Sciences Meeting Abstracts #49, 117.08
- Planetary Defense Interagency Working Group. 2023, National Preparedness Strategy & Action Plan for Near-Earth Object Hazards and Planetary Defense, Tech. rep., National Science & Technology Council, Office of Science and Technology Policy
- Porcello, L., Jordan, R., Zelenka, J., et al. 1974, *Proceedings of the IEEE*, 62, 769
- Rathbun, J. A., & Spencer, J. R. 2006, *Geophys. Res. Lett.*, 33, L17201
- Rathbun, J. A., Spencer, J. R., Davies, A. G., Howell, R. R., & Wilson, L. 2002, *Geophys. Res. Lett.*, 29, 1443
- Reddy, V., Kelley, M. S., Benner, L., et al. 2024, *Plan. Sci. J.*, 5, 141
- Rice, M., & Laughlin, G. 2019, *ApJ*, 884, L22
- Rivera-Valentín, E. G., Meyer, H. M., Taylor, P. A., et al. 2021, *Lunar and Planetary Science Conference*, 52, #2548
- Rivera-Valentín, E. G., Taylor, P. A., Rodriguez Sanchez-Vahamonde, C., et al. 2020, *Bulletin of the AAS*, 53
- Rivera-Valentín, E. G., Meyer, H. M., Taylor, P. A., et al. 2022, *Plan. Sci. J.*, 3, 62
- Rivkin, A. S., & Cheng, A. F. 2023, *Nature Communications*, 14, 1003
- Rivkin, A. S., Chabot, N. L., Stickle, A. M., et al. 2021, *Plan. Sci. J.*, 2, 173
- Rizos, J. L., de León, J., Pinilla-Alonso, N., et al. 2019, in *Ciencias Planetarias y Exploración del Sistema Solar*, 13
- Sánchez Net, M., Taylor, M., Vilnrotter, V., & Lazio, T. J. W. 2022, *The Interplanetary Network Progress Report*, 42-229, 1, https://ipnpr.jpl.nasa.gov/progress_report/42-229/42-229A.pdf
- Schilizzi, R. T., Alexander, P., Cordes, J. M., et al. 2007, Memo 100: Preliminary Specifications for the Square Kilometre Array, Tech. rep., International SKA Steering Committee
- Schwamb, M. E., Jones, R. L., Chesley, S. R., et al. 2018, arXiv e-prints, arXiv:1802.01783
- Shepard, M. K., Clark, B. E., Nolan, M. C., et al. 2008, *Icarus*, 195, 184
- Shepard, M. K., de Kleer, K., Cambioni, S., et al. 2021, *Plan. Sci. J.*, 2, 125
- Sherman, M. B., Connor, L., Ravi, V., et al. 2023, *ApJ*, 957, L8
- Slade, M. A., Butler, B. J., & Muhleman, D. O. 1992, *Science*, 258, 635
- Slade, M. A., Butler, B. J., & Muhleman, D. O. 1992, *Science*, 258, 635
- Smrekar, S., Hensley, S., Nybakken, R., et al. 2022, in *2022 IEEE Aerospace Conference (AERO)*, 1–20
- Stacy, N. J. S., Campbell, D. B., & Ford, P. G. 1997, *Science*, 276, 1527
- Statman, J. I., Bagri, D. S., Yung, C. S., Weinreb, S., & MacNeal, B. E. 2004, *Interplanetary Network Progress Report*, 42-159, 1
- Takir, D., & Emery, J. P. 2012, *Icarus*, 219, 641
- Tatsuuma, M., Kataoka, A., Tanaka, H., & Guillot, T. 2024, arXiv e-prints, arXiv:2407.21386

- Thomas, N., Sierks, H., Barbieri, C., et al. 2015, *Science*, 347, aaa0440
- Trumbo, S. K., Brown, M. E., & Butler, B. J. 2018, *AJ*, 156, 161
- Turtle, E. P., Perry, J. E., Hayes, A. G., et al. 2011, *Science*, 331, 1414
- Vander Hook, J., Doyle, R., Fox, V., & et al. 2021, *Nebulae: Deep-Space Computing Clouds*, Tech. rep., W. M. Keck Institute for Space Studies, Pasadena, CA, doi:10.7907/yqde-dj03
- Vander Hook, J., Castillo-Rogez, J., Doyle, R., et al. 2020, in *2020 IEEE Aerospace Conference (IEEE)*
- Vierinen, J., Tveito, T., Gustavsson, B., Kesaraju, S., & Milla, M. 2017, *Icarus*, 297, 179
- Vilnrotter, V., Giorgini, J., Jao, J., Lazio, J., & Snedeker, L. 2023, in *2023 IEEE Aerospace Conference*, 1–8
- Vilnrotter, V., Lee, D., Cornish, T., Mukai, R., & Paal, L. 2006, *Interplanetary Network Progress Report*, 42-166, 1
- Vilnrotter, V., Lee, D., Cornish, T., et al. 2009, in *2009 IEEE Aerospace Conference*, 1–8
- Vilnrotter, V., Lee, D., Cornish, T., et al. 2010a, *IEEE Aerospace and Electronic Systems Magazine*, 25, 29
- Vilnrotter, V., Lee, D., Tsao, P., Cornish, T., & Paal, L. 2010b, in *2010 IEEE Aerospace Conference*, 1–12
- Vilnrotter, V., Tsao, P., Lee, D., et al. 2011, in *2011 Aerospace Conference*, 1–13
- Virkki, A., Zubko, E., Nolan, M. C., et al. 2019, *Icarus*, 325, 94
- Virkki, A. K., Neish, C. D., Rivera-Valentín, E. G., et al. 2023, *Remote Sensing*, 15, 5605
- Walsh, K. J., Morbidelli, A., Raymond, S. N., O’Brien, D. P., & Mandell, A. M. 2011, *Nature*, 475, 206
- Wang, N., Xu, Q., Ma, J., et al. 2023, *Science China Physics, Mechanics, and Astronomy*, 66, 289512
- Wilkinson, S. R., Hansen, C., Alexia, B., et al. 2022, *Microwave J.*, 65, <https://www.microwavejournal.com/articles/37417-a-planetary-radar-system-for-detection-and-high-resolution-imaging-of-nearby-celestial-bodies>
- Zhang, Z., Brown, S., Bolton, S., et al. 2023, *Geophys. Res. Lett.*, 50, e2022GL101565